Further Development of Verification Check-cases for Six-Degree-of-Freedom Flight Vehicle Simulations

E. Bruce Jackson[*] and Michael M. Madden[†]
NASA Langley Research Center, Hampton, VA 23681, USA

Dr. Robert Shelton[‡] and Dr. A. A. Jackson[§]
NASA Johnson Space Center, Houston, TX 77058, USA

Manuel P. Castro[**] and Deleena M. Noble[**]
NASA Armstrong Flight Research Center, Edwards, CA 93523, USA

Curtis J. Zimmerman[††]
NASA Marshall Space Flight Center, Huntsville, AL 35812, USA

Jeremy D. Shidner[‡‡], Joseph P. White[§§], Soumyo Dutta[***], Eric M. Queen[***], Richard W. Powell[‡‡], William A. Sellers[†††], Scott A. Striepe[‡‡‡], and John Aguirre[§§§]
NASA Langley Research Center, Hampton, VA 23681, USA

Nghia Vuong[****], Scott E. Reardon[††††], Michael J. Weinstein[††††] and William Chung[‡‡‡‡]
NASA Ames Research Center, Mountain View, CA 94035, USA

and

Jon S. Berndt[§§§§]
JSBSim Open Source Project, Westminster, CO 80027, USA

This follow-on paper describes the principal methods of implementing, and documents the results of exercising, a set of six-degree-of-freedom rigid-body equations of motion and planetary geodetic, gravitation and atmospheric models for simple vehicles in a variety of endo- and exo-atmospheric conditions with various NASA, and one popular open-source, engineering simulation tools. This effort is intended to provide an additional means of verification of flight simulations. The models used in this comparison, as well as the resulting time-history trajectory data, are available electronically for persons and organizations wishing to compare their flight simulation implementations of the same models.

[*] Sr. Aerospace Engineer, Dynamic Systems and Control Branch, MS 308, AIAA Associate Fellow.
[†] Chief Scientist, Simulation Development and Analysis Branch, MS 125B, AIAA Senior Member.
[‡] Lead, JSC Engineering Orbital Dynamics (JEOD), Engineering Directorate, Mail Code ER7.
[§] Sr. Engineer, Jacobs Engineering Group, Inc., Engineering Directorate, AIAA Associate Fellow.
[**] Aerospace Engineer, AFRC Simulation Engineering, MS 4840.
[††] Aerospace Engineer, Guidance, Navigation and Mission Analysis Branch, MSFC/EV42, AIAA Member.
[‡‡] Aerospace Engineer, Analytical Mechanics & Assoc., MS 489, Associate Fellow (Powell); Sr. Member (Shidner).
[§§] Senior Project Engineer, Analytical Mechanics & Associates, MS 489.
[***] Aerospace Engineer, Atmos. Flight & Entry Systems Branch, MS 489, Sr. Member (Queen), Member (Dutta).
[†††] Senior Systems Analyst, Stinger Ghaffarin Technologies, Inc., MS 489, AIAA Member.
[‡‡‡] Aerospace Engineer, Atmospheric Flight & Entry Systems Branch, MS 489.
[§§§] Scientific Programmer, Analytical Mechanics & Associates, MS 489.
[****] Systems Software Engineer, Aerospace Sim. Research & Development Branch, MS 243-5, AIAA Member.
[††††] Flight Simulation Engineer, Aerospace Sim. Research & Development Branch, MS 243-5, AIAA Member.
[‡‡‡‡] Sr. Simulation Engineer, SAIC, Aerospace Sim. Res. & Devel. Branch, MS-243-6, Associate Fellow.
[§§§§] Project Lead, Member.

I. Nomenclature

C_D	=	*Aerodynamic drag coefficient*
F	=	*Force*
h	=	*Geometric altitude*
J_2	=	*Second degree zonal harmonic coefficient of gravitation*
R	=	*Radius to center of Earth*
T	=	*Torque*
t	=	*Time*
x	=	*Body longitudinal axis, +forward*
y	=	*Body lateral axis, +right to an observer facing in positive x direction*
Z	=	*Geopotential height*
z	=	*Body vertical axis, +down*

Acronymns

6-DOF	=	*Six-degree-of-freedom*
CM	=	*Center of Mass*
CSV	=	*Comma-Separated Values*
DAVE-ML	=	*Dynamic Aerospace Vehicle Exchange Markup Language*
DOF	=	*Degrees-of-freedom*
ECEF	=	*Earth-centered, earth-fixed (rotating coordinate frame)*
ECI	=	*Earth-centered inertial (non-rotating coordinate frame)*
EOM	=	*Equations of Motion*
GEM-T1	=	*Goddard Earth Model T1*
ISS	=	*International Space Station*
J2000	=	*Earth-centered inertial frame for epoch 2000*
JEOD	=	*JSC Engineering Orbital Dynamics*
JSBSim	=	*Open-source, data-driven, simulation framework in C++*
kt	=	*knots (nautical miles per hour)*
LaSRS++	=	*Langley Standard Real-time Simulation in C++*
LVLH	=	*Local Vertical, Local Horizontal frame*
MAVERIC	=	*Marshall Aerospace Vehicle Representation in C*
MET	=	*Marshall Engineering Thermosphere*
MRC	=	*Moment Reference Center*
NED	=	*North-East-Down*
NESC	=	*NASA Engineering and Safety Center*
POST II	=	*Program to Optimize Simulated Trajectories II*
S-119	=	*ANSI/AIAA S-119-2011 Flight Dynamic Model Exchange Standard*
Unicode	=	*Uniform character encoding standard*
URL	=	*Uniform Resource Locator*
VMSRTE	=	*Vertical Motion Simulator Real-Time Environment*
WGS-84	=	*World Geodetic System 1984*
XML	=	*eXtensible Markup Language*

I. Introduction

THE rise of innovative unmanned aeronautical systems and the emergence of commercial space activities have resulted in a number of relatively new aerospace organizations that are designing innovative systems and solutions. These organizations use a variety of commercial off-the-shelf and in-house-developed simulation and analysis tools including 6-degree-of-freedom (6-DOF) flight simulation tools. The increased affordability of computing capability has made high-fidelity flight simulation practical for all participants. Verification of the tools' equations-of-motion and environment models (e.g., atmosphere, gravitation, and geodesy) is desirable to assure accuracy of results. However, aside from simple textbook examples, minimal verification data exists in open literature for 6-DOF flight simulation problems.

This paper compares multiple solution trajectories to a set of verification check-cases that covered atmospheric and exo-atmospheric (i.e., orbital) flight. Each scenario consisted of pre-defined flight vehicles, initial conditions,

and maneuvers. These scenarios were implemented and executed in a variety of analytical and real-time simulation tools. This tool-set included simulation tools in a variety of programming languages based on modified flat-Earth, round-Earth, and rotating oblate spheroidal Earth geodesy and gravitation models, and independently derived equations-of-motion and propagation techniques. The resulting simulated parameter trajectories were compared by over-plotting and difference-plotting to yield a family of solutions.

In total, seven simulation tools were exercised. Participating in this exercise were participants from NASA Ames Research Center (ARC), Armstrong Flight Research Center (AFRC), Johnson Space Center (JSC), Langley Research Center (LaRC), and Marshall Space Flight Center (MSFC), and an open-source simulation tool development project (i.e., JSBSim).

The vehicle models defined by the check-cases were published in the American Institute of Aeronautics and Astronautics/American National Standards Institute (AIAA/ANSI) S-119-2011 Flight Dynamics Model Exchange Standard (S-119) markup language[1], making them realizable in a variety of proprietary and non-proprietary implementations. This set of models and the resulting trajectory plots from a collection of simulation tools may serve as a preliminary verification aide for organizations that are developing their own atmospheric and orbital simulation tools and frameworks. The models and trajectory data are available from the NASA Engineering and Safety Center's (NESC) Academy website, in the Flight Mechanics area[2]. This exercise is believed to be the first publically available comparison of a set of 6-DOF flight simulation tools. An earlier NASA study[4] compared exo-atmospheric scenarios between NASA and international space agency partners, but those results are not publically available.

An earlier paper reported on preliminary results of this effort that included mostly simple check-cases; this paper presents the final results of this multiyear effort involving additional, more complex, vehicle models and maneuvers. Models and data sets associated with this effort are available on-line for others to use for comparison with additional simulation tools.[3]

II. Approach

The NESC's Technical Fellow for Flight Mechanics assembled a team to develop flight simulation verification data sets. This team mapped out an approach to developing check-cases for comparison and cross-verification purposes.

The team agreed that a set of scenarios involving simple models would be developed and simulated by each participant in their preferred simulation tool. In an attempt to build a "consensus" solution for 6-DOF flight vehicle simulations, a set of relatively simple flight vehicle models was developed, with a set of maneuvers from specified initial conditions, in a variety of atmospheric, gravitational, and geodetic configurations. It was anticipated the resulting trajectories would fall into one or more families of solutions based upon assumptions and simplifications (e.g., flat-Earth conditions). The basic parameters were agreed upon and further discussion led to the set of scenarios described in Section II.H. Formats for specifying the models, initial conditions, and resulting time-history data were agreed to and a plan for presenting the data was developed.

Instead of identifying a single "known good" simulation tool, or requiring that all "good" trajectories match within a predefined tolerance, the approach taken was to present comparison plots of the results of each simulation tools. If acceptable agreement between the parameter trajectories generated by the tools was found, then those trajectories could serve as a verification guide. If unacceptable difference in results was evident, then an attempt would be made to identify an assumption, design choice, and/or an implementation difference to explain the disparity, and the set of trajectories would serve as a family of possible solutions. (For this purpose, the term "acceptable agreement" remained a subjective concept.)

One of the overall objectives was to generate a publically available report containing the salient results for use by current and future organizations. Furthermore, it was desirable to make the vehicle models and resulting trajectory data available electronically for ease of comparison by developers of other simulation tools.

A. Check-Case Vehicle Models

A set of reference flight vehicles was proposed, based primarily on existing non-proprietary vehicle models. For the atmospheric scenarios, the "vehicles" included a spheroid (i.e., cannonball), a brick to evaluate rotational dynamics, a subsonic fighter with representative nonlinear aerodynamics, propulsion, and control law models, and a two-stage rocket. For the orbital cases, a larger spheroid, a cylindrical rocket body, and a simplified International Space Station (ISS) models were re-used from an earlier comparison study[4].

B. Check-Case Geodesy Models

One of the challenges in performing 6-DOF flight simulations is the choice in how to model the Earth's shape and motion. Early low-speed atmospheric flight simulations often used a flat-Earth approximation that was sufficient for recreating landing and takeoff dynamics. Early computational performance limitations made this simplifying approximation attractive for pilot-in-the-loop ("real-time") training or research and development simulations.

As digital computers grew in capability, simulation of flight using more accurate spherical and oblate rotating Earth models became practical from a cost/time standpoint. Many atmospheric flight simulation tools incorporated the standard DoD World Geodetic System 1984 (WGS-84)[5] ellipsoidal Earth model even though an iterative solver, or other multi-step iterative process, was normally required to convert between inertial coordinates and geodetic coordinates (i.e., latitude, longitude, and altitude) with the ellipsoidal geodesy model.

The atmospheric check-case scenarios developed for this study included round non-rotating, round rotating, and ellipsoidal rotating Earth models. The orbital check-case scenarios used the oblate WGS-84 model exclusively.

C. Check-Case Coordinate Systems

A number of coordinate system definitions and transformations were required in this exercise including: J2000 inertial; Earth-centered inertial (ECI); Earth-centered Earth-fixed (ECEF) in either geocentric or geodetic frames; local-vertical, local-horizontal (LVLH); north-east-down (NED); launch site; and body coordinates.

D. Check-Case Gravitation Models

In parallel with a choice of Earth geodesy models was a corresponding choice of gravitation models. The simplest model had gravitational attraction varying inversely with the square of the vehicle distance from Earth's center. This simplified model is often used with the approximation of a spherical Earth.

A more sophisticated gravitation model, including gravitational harmonics that vary with latitude and longitude, is normally employed for ellipsoidal Earth models. For atmospheric check-cases with a WGS-84 Earth, the first non-zero term of the harmonic series (i.e., J_2 gravitation) is included. Orbital scenarios included the J_2 and higher harmonic terms (i.e., to 8×8) using the Goddard Earth Model (GEM)-T1 harmonic coefficients[6].

E. Check-Case Atmosphere Models

US 1976. The US Standard 1976 Atmosphere model[7] was used for the majority of the atmospheric check-case scenarios. This model can be implemented as linear interpolation of the one-dimensional tables given in the source document with ambient pressure, temperature, and density as a function of geometric altitude (h) or geopotential height (Z). A more accurate implementation was to realize atmospheric properties directly from the non-linear numerical equations used to generate the tables published in reference 7.

Marshall Engineering Thermosphere (MET). The MET is appropriate for modeling the thermosphere region of the Earth's atmosphere, located above the stratosphere (i.e., greater than 90 km) but below the exosphere (i.e., less than 500 km). MET is employed for most of the orbital check-cases. This model is not publicly available, but can be requested from the MSFC Natural Environments Branch.

F. Check-Case Data Formats

The use of standard formats should significantly shorten the process of sharing models and comparing results. While some setup was required for each tool to receive models in an unfamiliar format and translate the data in a locally-compatible format, it was hoped the ability to quickly implement model changes and generate new results would be enhanced by this investment.

Reference models. Most of the atmospheric check-cases vehicle models were specified using the format in Ref. 1 (i.e., S-119), which makes use of an extensible markup language (XML) based grammar, DAVE-ML[8]. This format attempted to encode the salient flight characteristics of an aerospace vehicle (i.e., aerodynamic and inertial properties) unambiguously in a text file that is human- and machine-readable, and with sufficient metadata to be easily converted into code and to be readily archivable. The most complex model attempted in this study was the single-engine F-16 aircraft defined in DAVE-ML using S-119 variable names that included an inertial/mass properties model, a non-linear aerodynamic model, and two separate control law subsystem models. These models are available from the NESC Academy website (Ref 2).

Time-History Data. Despite an attempt to identify a more efficient binary data format for the several million data points that were generated in this effort, the team eventually stored data in a comma-separated-values (.CSV) text format. These files used column headers to identify the values represented and rows to group values associated with regular time steps of simulation. The check-case files were large (e.g., 12 MB in one case) as a result of using

text instead of binary value representations, but this format was felt to be better suited for archival purposes and to be more readily accessible by other reviewers. The time-history data files are also available from the NESC Academy website (Ref. 2).

G. Participating Simulation Tools

Developers of several NASA and one open-source simulation tools agreed to participate in this comparison on a voluntary basis. The set of tools involved included simulations suited primarily for atmospheric flight, exo-atmospheric flight, and some were applicable to both flight regimes. Not all simulation tools attempted to execute every check-case. The team agreed to a ground rule that a minimum of three data sets (i.e., parameter trajectories) generated by independent tools were necessary to warrant inclusion in this exercise.

The assembled tool-set included:

- Core from ARFC
- JEOD from JSC
- JSBSim (open source EOM)
- LaSRS++ from LaRC
- MAVERIC from MSFC
- POST II from LaRC
- VMSRTE from ARC

The resulting data-sets cited later in this report are identified anonymously as resulting from "SIM 1" or "SIM A"; this is intentional to encourage participation and comparison between tool providers.

H. Check Case Scenarios

A set of atmospheric and orbital flight scenarios, models, and initial conditions was developed by the team (see Table 1 and Table 2). Seventeen atmospheric check cases were identified and sixteen cases were run with at least three simulation tools (one case, number 14, was also run by three simulation tools, but was not included in the exercise due to lack of agreement on test inputs). Twenty-six orbital check cases were identified and all were run with at least three simulation tools.

III. Illustrative Samples from Comparison

Key parameters were compared by mapping each simulation tool's preferred variable name into the S-119 standard naming scheme and were both over- and difference-plotted. Table 3 lists the parameters that were compared along with their definitions, dimensionality and units of measure.

Table 1. Atmospheric Check Case Scenarios

Number	Name	Verifies	Gravitational	Geodesy	Winds
1	Dropped sphere with no drag	Gravitation, translational EOM	J_2	WGS-84	Still air
2	Tumbling brick with no damping, no drag	Rotational EOM	J_2	WGS-84	Still air
3	Tumbling brick with dynamic damping, no drag	Inertial coupling	J_2	WGS-84	Still air
4	Dropped sphere with constant C_D, no wind	Gravitation, integration	$1/R^2$	Round fixed	Still air
5	Dropped sphere with constant C_D, no wind	Earth rotation	$1/R^2$	Round rotating	Still air
6	Dropped sphere with constant C_D, no wind	Ellipsoidal Earth	J_2	WGS-84	Still air
7	Dropped sphere with constant C_D + wind	Wind effects	J_2	WGS-84	Steady wind
8	Dropped sphere with constant C_D + wind shear	2 dimensional wind	J_2	WGS-84	$f(h)$
9	Sphere launched eastward along equator	Translational EOM	J_2	WGS-84	Still air
10	Sphere launched northward along prime meridian	Coriolis	J_2	WGS-84	Still air
11	Subsonic F-16 trimmed flight across planet	Atmosphere, air-data calculations	J_2	WGS-84	Still air
12	Supersonic F-16 trimmed flight across planet	Supersonic air-data calculations	J_2	WGS-84	Still air
13	Subsonic F-16 maneuvering flight	Multidimensional table look-up	J_2	WGS-84	Still air
14	Supersonic F-16 maneuvering flight (not completed)	Mach effects in tables	J_2	WGS-84	Still air
15	Circular F-16 flight around North pole	Propagation, geodetic transforms	J_2	WGS-84	Still air
16	Circular F-16 flight around equator/dateline intersection	Sign changes in latitude and longitude	J_2	WGS-84	Still air
17	Two-stage rocket to orbit	Staging, entire atmosphere	J_2	WGS-84	$f(h)$

Table 2. Exo-Atmospheric Check Case Scenarios

Number	Name	Verifies	Gravitation	3rd body pert.	Body
1	Earth Modeling Parameters	Environmental constants	$1/R^2$	None	ISS
2	Keplerian Propagation	Integration, rotation-nutation precession, orientation	$1/R^2$	None	ISS
3A	Gravitation Modeling: 4 × 4	4 × 4 harmonic gravitation model	4 × 4	None	ISS
3B	Gravitation Modeling: 8 × 8	8 × 8 harmonic gravitation model	8 × 8	None	ISS
4	Planetary Ephemeris	Third body gravitational forces	$1/R^2$	Sun, moon	ISS
5A	Minimum Solar Activity	Free molecular flow	$1/R^2$	None	ISS
5B	Mean Solar Activity	Free molecular flow	$1/R^2$	None	ISS
5C	Maximum Solar Activity	Free molecular flow	$1/R^2$	None	ISS
6A	Constant Density Drag	Response to constant force	$1/R^2$	None	Sphere
6B	Aero Drag with Dyn. Atmos.	Response to dynamic drag	$1/R^2$	None	Sphere
6C	Plane Change Maneuver	Response to propulsion firing	$1/R^2$	None	Cylinder
6D	Earth Departure Maneuver	Response to propulsion firing	$1/R^2$	None	Cylinder
7A	4 × 4 gravitation	Translation response	4 × 4	Sun, moon	Sphere
7B	8 × 8 gravitation	Translation response	8 × 8	Sun, moon	Sphere
7C	All Models with 4 × 4 gravitation	Translation response	4 × 4	Sun, moon	Sphere
7D	All Models with 8 × 8 gravitation	Translation response	8 × 8	Sun, moon	Sphere
8A	Zero Initial Attitude Rate	Integration methods for rotation	$1/R^2$	None	ISS
8B	Non-Zero Initial Attitude Rate	Integration methods for rotation	$1/R^2$	None	ISS
9A	Zero Initial Rate w/ Torque (T)	Rotational response	$1/R^2$	None	ISS
9B	Non-Zero Initial Rate w/ Torque	Rotational response	$1/R^2$	None	ISS
9C	Zero Initial Rate w/ T + Force (F)	Rotational response	$1/R^2$	None	ISS
9D	Non-Zero Initial Rate w/ $T + F$	Rotational response	$1/R^2$	None	ISS
10A	Zero Initial Attitude Rate	Gravity gradient modeling	$1/R^2$	None	Cylinder
10B	Non-Zero Initial Rate	Gravity gradient modeling	$1/R^2$	None	Cylinder
10C	Zero Initial Rate; Elliptical Orbit	Gravity gradient modeling	$1/R^2$	None	Cylinder
10D	Non-Zero Initial Rate; Ellip. Orbit	Gravity gradient modeling	$1/R^2$	None	Cylinder
FULL	Integrated 6-DOF Orbital Motion	Combined effects response	8 × 8	Sun, moon	ISS

Table 3. Compared parameter names

Parameter label	Units	Size	Description (sign convention)
`aero_bodyForce`	lbf	3-vector	Aerodynamic forces resolved into body x-y-z axes
`aero_bodyMoment`	ft-lbf	3-vector	Aerodynamic moments about the center of mass, resolved into body x-y-z axes
`airDensity`	kg/m^3 or $slug/ft^3$	scalar	Atmospheric density
`altitudeMsl`	ft or m	scalar	Geometric altitude above reference ellipsoid sphere or plane
`altitudeRateWrtMsl`	ft/min	scalar	Rate of climb relative to reference surface (+up)
`ambientPressure`	lbf/ft^2	scalar	Atmospheric (static) pressure
`ambientTemperature`	K or °R	scalar	Atmospheric (static) temperature
`bodyAngularRateWrtEi`	rad/s or deg/s	3-vector	Pitch, roll and yaw rates around body x-y-z axes with respect to ECI frame
`bodyLocalGravitation`	m/s^2	3-vector	Gravitational acceleration resolved into body x-y-z axes
`dynamicPressure`	lbf/ft^2	scalar	Dynamic pressure due to relative motion between vehicle and the surrounding atmosphere
`eiAccel`	m/s^2	3-vector	Acceleration of the vehicle's center of mass with respect to the ECI frame, resolved in ECI X-Y-Z axes
`eiPosition`	ft or m	3-vector	Position of the vehicle's center of mass with respect to the ECI frame, resolved in the ECI X-Y-Z axes
`eiVelocityWrtEi`	ft/s or m/s	3-vector	Velocity of the vehicle's center of mass with respect to the ECI frame, resolved in the ECI X-Y-Z axes
`eiVelocity`	ft/s or m/s	3-vector	Velocity of the vehicle's center of mass with respect to the ECI frame, resolved in the ECI X-Y-Z axes
`eulerAngle`	deg or rad	3-vector	Attitude of the vehicle with respect to the LVLH frame (orbital check-cases) or NED frame (atmospheric check-cases), resolved into pitch, roll and yaw angles using a 3-2-1 sequence
`feVelocity`	ft/s	3-vector	Velocity of the vehicle's center of mass with respect to the flat-earth frame, resolved in the N-E-D axes
`gast`	rad	scalar	Rotation angle of Earth (Greenwich Apparent Sidereal Time)
`gePosition`	ft or m	3-vector	Position of the vehicle's center of mass with respect to the ECEF frame, resolved in the ECEF X-Y-Z axes
`latitude`	deg	scalar	Position of the vehicle's center of mass given as the geodetic latitude
`localGravity`	ft/s^2	scalar	Gravitational acceleration of the vehicle's center of mass in the local 'down' direction
`longitude`	deg	scalar	Position of the vehicle's center of mass given as the geodetic longitudinal
`mach`	--	scalar	Mach number
`speedOfSound`	ft/s	scalar	Sonic velocity in the atmosphere at the current altitude
`trueAirspeed`	nmi/h (kt)	scalar	Velocity of the vehicle's center of mass with respect to the surrounding atmosphere

A. Atmospheric Check-case Examples

Three scenarios, two atmospheric and one orbital, were selected to illustrate the similarities and differences among the simulations that were typical for the full set of check-cases. The complete time-history results for all 17 check-cases are available for download (see Ref. 3) and are fully discussed in Ref. 9.

1. Simple Vehicle Check Case

In this selected scenario, the sphere was launched eastward from the equator/prime meridian intersection, starting at sea level, with an initial 45° vertical flight path angle as specified in table 4. The sphere's body x-axis was aligned eastward with zero pitch or roll angle with respect to the launch point. There is no relative rotation with respect to the launch point.

Table 4. Initial conditions for atmospheric scenario 9

Scenario	9: Sphere launched ballistically eastward along the equator			
Vehicle	Sphere with constant C_D			
Geodesy	WGS-84 rotating			
Atmosphere	US 1976 STD; no wind			
Gravitation	$J2$		**Duration**	30 s
Initial states	**Position** (deg, deg, ft msl)	**Velocity** ft/s	**Attitude** deg	**Rate** deg/s
Geodetic Local-relative Body axes	[0, 0, 0]	[0, 1000, -1000]	[0, 0, 90]	[0, 0, 0]
Notes	Initial velocity is $\sqrt{2,000,000}$ ft/s aligned 45° from vertical, heading East; zero angular rate relative to launch platform			

Figure 1 through Figure 7 compare results between six simulation tools, as well as the deviances of the outputs from each tool from the ensemble average value.

This scenario launched the sphere on a ballistic trajectory to the east along the equator. The sphere had zero initial Earth-relative velocity and angular rates. However, it developed a pitch relative to the Earth due to the eastward travel. In fact, the change in pitch angle should have been exactly equal to the change in longitude.

Of the five simulation tools that attempted this check-case, four showed this equivalence between longitude and pitch angle differences, with the exception being SIM 2 (see Figure 2 and Figure 3). As detailed in ref. 9, integration error differences for the Euler angles had been identified for SIM 2 in atmospheric scenario 2, it was assumed that the pitch angle difference shown for SIM 2 was due to a combination of this difference in integration methods and in the longitude traveled. In any case, the differences in pitch angle were not significant for the duration of this scenario.

The differences in translational motion were larger. The simulations all agreed that no motion occurs to the north. But simulations differed on the amount of travel eastward and upward by nearly 5 feet at t = 30 s. SIM 4, 5, and 6 closely agreed on gravitation, aerodynamic forces, translational velocity, and position; therefore, these simulations were used as a basis for discussing differences among the remaining simulations. (This was not an endorsement that these simulations produce the "correct" result; this simply reduced the number of differences to analyze.)

First, the external forces were examined for the contributors to differences in translational motion. The difference plot for local gravity (Figure 4) did portray a jump in the gravitational difference in SIM 1 and SIM 2 at t = 0.1 s. These differences in gravitation would require geopotential altitude differences of about −10 and −3.5 feet respectively when compared to SIM 3, 4, 5, and 6. However, the altitude difference plot did not show any visible difference in altitude at t = 0.1 s. An alternative explanation is a delay in recording gravitation, e.g. the higher gravitational value corresponded to the lower altitude of a previous frame. This explanation matched well with the difference seen in SIM 2 if the recording delay was 0.01 seconds. The initial upward velocity of the sphere was 1,000 ft/s; therefore, a delay of 0.01 s in recording represented nearly a −10 ft altitude bias in the gravitation reported at simulation start. Moreover, since gravitation and aerodynamic drag would reduce the upwards velocity over time, the altitude bias in the reported gravity that was associated with a 0.01 s lag should decline, at least until the sphere begins to accelerate back towards the Earth's surface. At t = 30 s, the sphere had passed the apex in its

trajectory but the downward velocity remained low. The altitude bias for a 0.01 s delay would be +1.8 ft. However, at the same time, SIM 2 showed an altitude difference that had grown to approximately 1.4 feet, relative to the consensus group (SIM 4/5/6) (Figure 2). The altitude difference, therefore, largely canceled the altitude bias from the recording lag and the difference in gravitation between SIM 2 and SIM 4/5/6 at t = 30 seconds was reduced to nearly zero, as shown on the plots (Figure 4). The "recording delay" also appeared to explain the gravitation differences in SIM 1 but the required delay would have needed to be about 0.004 s which is not a frame rate reported by the simulation. Furthermore, SIM 1 did not exhibit a steady decline in gravitation difference; instead, the gravitation difference exhibited a slight increase over time (Figure 4). This likely occurred because the altitude difference between SIM 1 and SIM 4/5/6 was increasing in a direction that initially compensates for and then exceeded the decline in the lag-induced altitude bias.

Remaining differences in gravitation among the simulations were consistent with the plotted differences in altitude. In any case, even if the largest gravitation differences (which appeared to be due to recording delay) were applied to the EOM, they would account for differences in downward-axis velocity and altitude of less than 0.0005 ft/s and 0.009 ft, respectively, at t = 30 seconds. Thus, gravitation differences were not a driving contributor to differences in translational motion.

Differences in aerodynamic forces were larger than those for gravitation. The differences in SIM 2 aerodynamic forces had two main contributors, a 0.01 s delay in the recorded forces and a difference in atmospheric density. The delay was a recording artifact only and did not contribute to differences in velocity and position. The difference in atmospheric density derived from implementing the atmosphere model using a lookup table (Figure 7). From the data, it appears that SIM 2 used 1,000 m for the first break-point but every break-point thereafter was at 500 m increments. Small aerodynamic force differences (Figure 1) arising from differences in atmospheric density were the primary contributor for differences in translational motion between SIM 2 and SIM 4/5/6; they accounted for nearly all of the differences in velocity (Figure 5) and position (Figure 2) relative to SIM 4/5/6.

SIM 1 also used a lookup table to estimate atmospheric density; the lookup table has 1000 m breakpoints throughout the altitudes traversed in this case (Figure 7). The density difference was the primary contributor to the difference in aerodynamic forces between SIM 1 and SIM 4/5/6 (Figure 1). The evolving difference in velocity was a secondary contributor (Figure 5). However, the aerodynamic force differences for SIM 1 would only account for only 61% of the eastward velocity and longitude differences, 34% of the downward velocity difference, and 46% of the altitude difference.

The source of the remaining difference between SIM 1 and the SIM 4/5/6 group in translational motion could not be identified from the recorded data. The remaining contributor is likely an unknown difference in EOM implementation or configuration possibly including, but not limited to, differences in integration or other numerical methods.

Differences in aerodynamic forces (Figure 1) in SIM 3 were largely a response to the growing differences in velocity and altitude (which determined atmospheric density). A small difference in orientation of SIM 3 relative to SIM 4/5/6 also contributed to the differences in aerodynamic forces. Although SIM 3 values for Euler angles are not plotted, the SIM 3 data file had a very small initial roll angle (-6.4×10^{-6} degrees). This small roll angle likely explained the difference of order 1×10^{-7} lbf seen in body y-axis aerodynamic force (Figure 1). Nevertheless, the orientation difference did not contribute to differences in translational velocity and position. Relative to SIM 4/5/6, the expected contributions of the aerodynamic force differences to differences in translational motion at t = 30 seconds were +0.14 ft/s in eastward velocity, $+6.4\times10^{-6}$ degrees in longitude, −0.098 ft/s in downward velocity, and +1.8 ft in altitude. However, the total differences were larger and in the opposite direction. They were −0.16 ft/s in eastward velocity, -1.4×10^{-5} degrees in longitude, +0.14 ft/s in downward velocity, and −4.3 ft in altitude. As with SIM 2, the additional contributor(s) to these small differences could not be identified using the recorded data; it is also likely an unknown difference in EOM implementation or configuration including, but not limited to, differences in integration or other numerical methods.

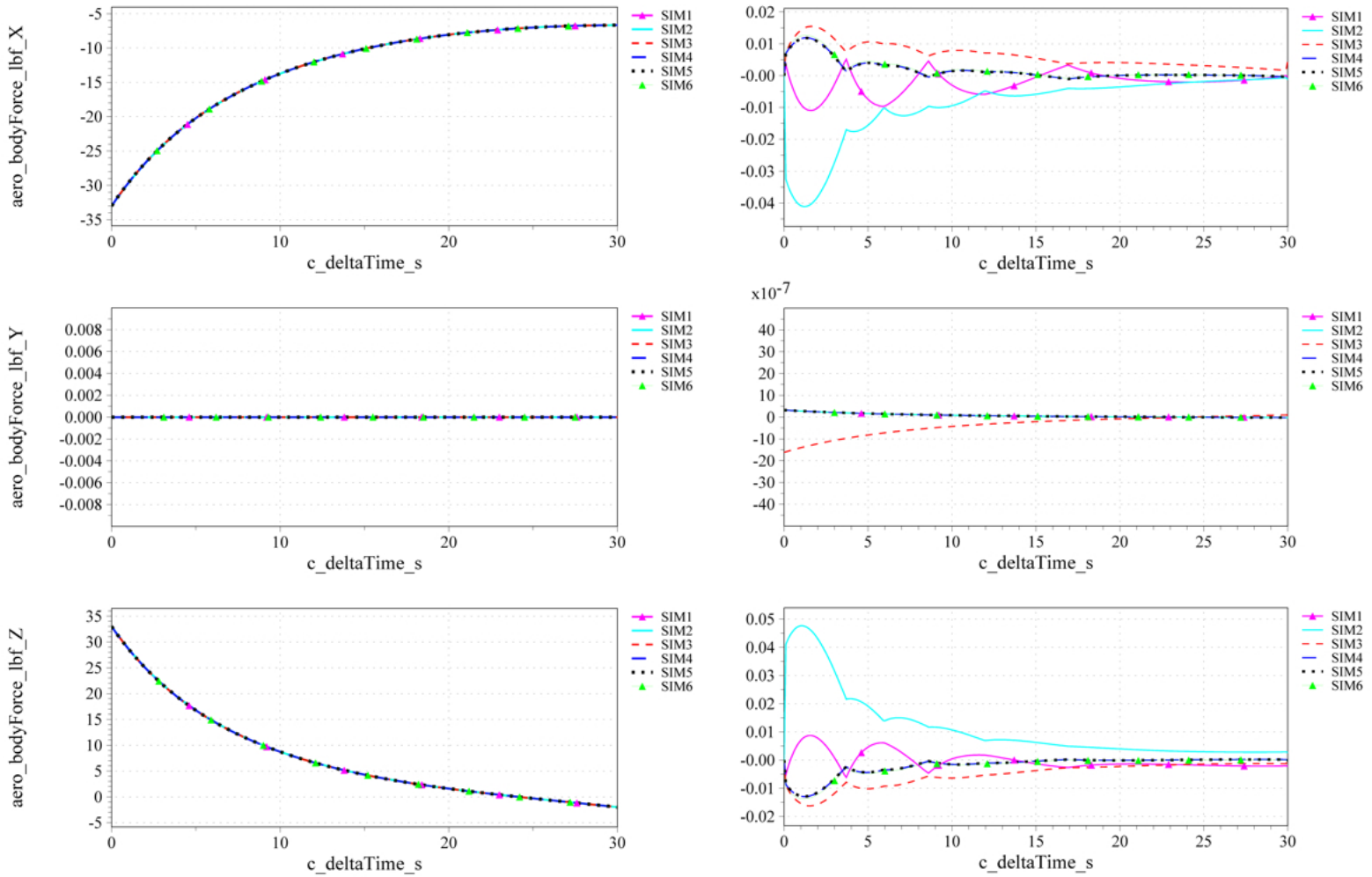

(a) Comparison of Aerodynamic Forces

(b) Differences in Aerodynamic Forces

Figure 1. Atmospheric Scenario 9 Results for Aerodynamic Forces

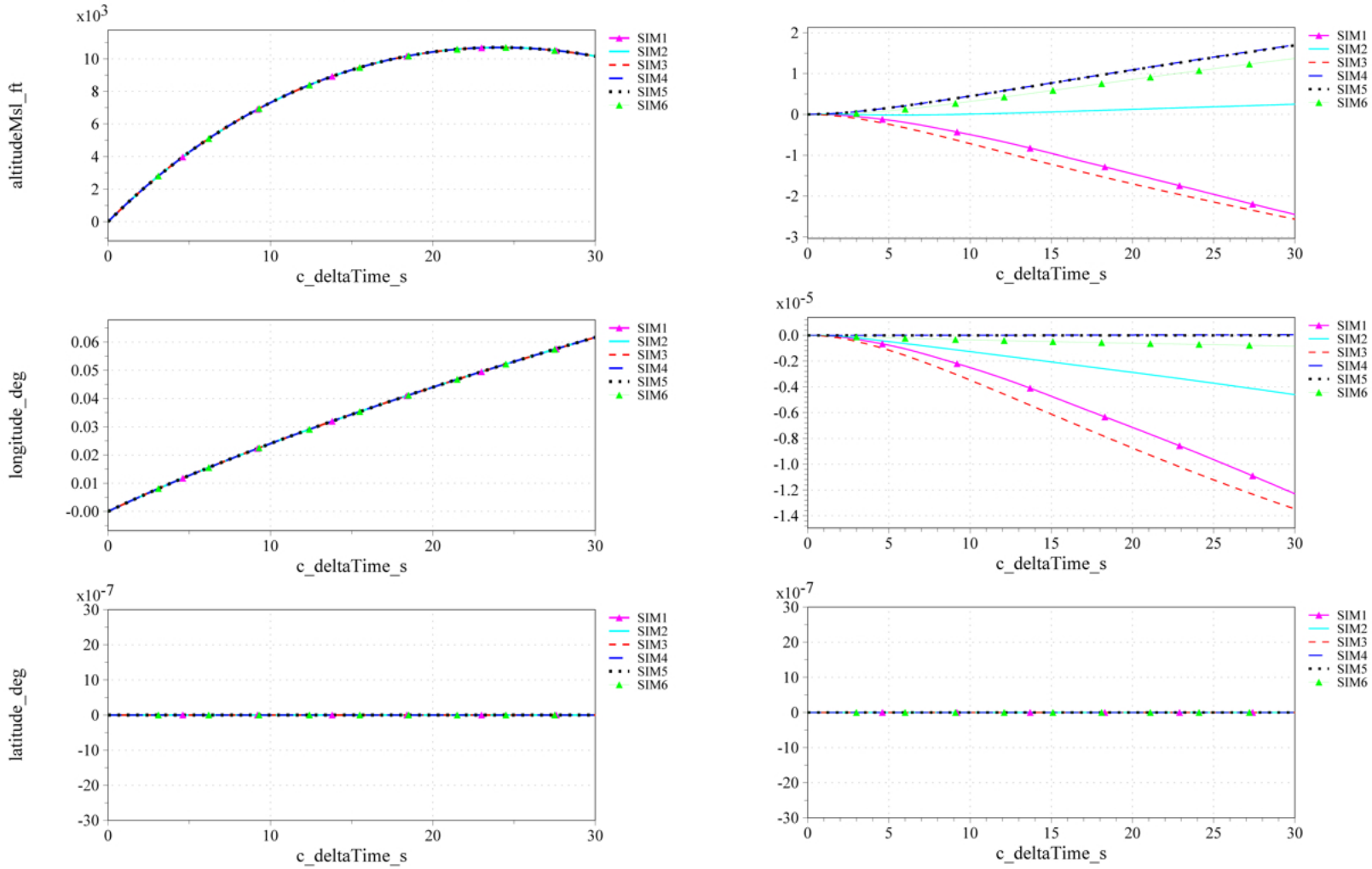

(a) Comparison of Geodetic Position

(b) Differences in Geodetic Position

Figure 2. Atmospheric Scenario 9 Results for Geodetic Position

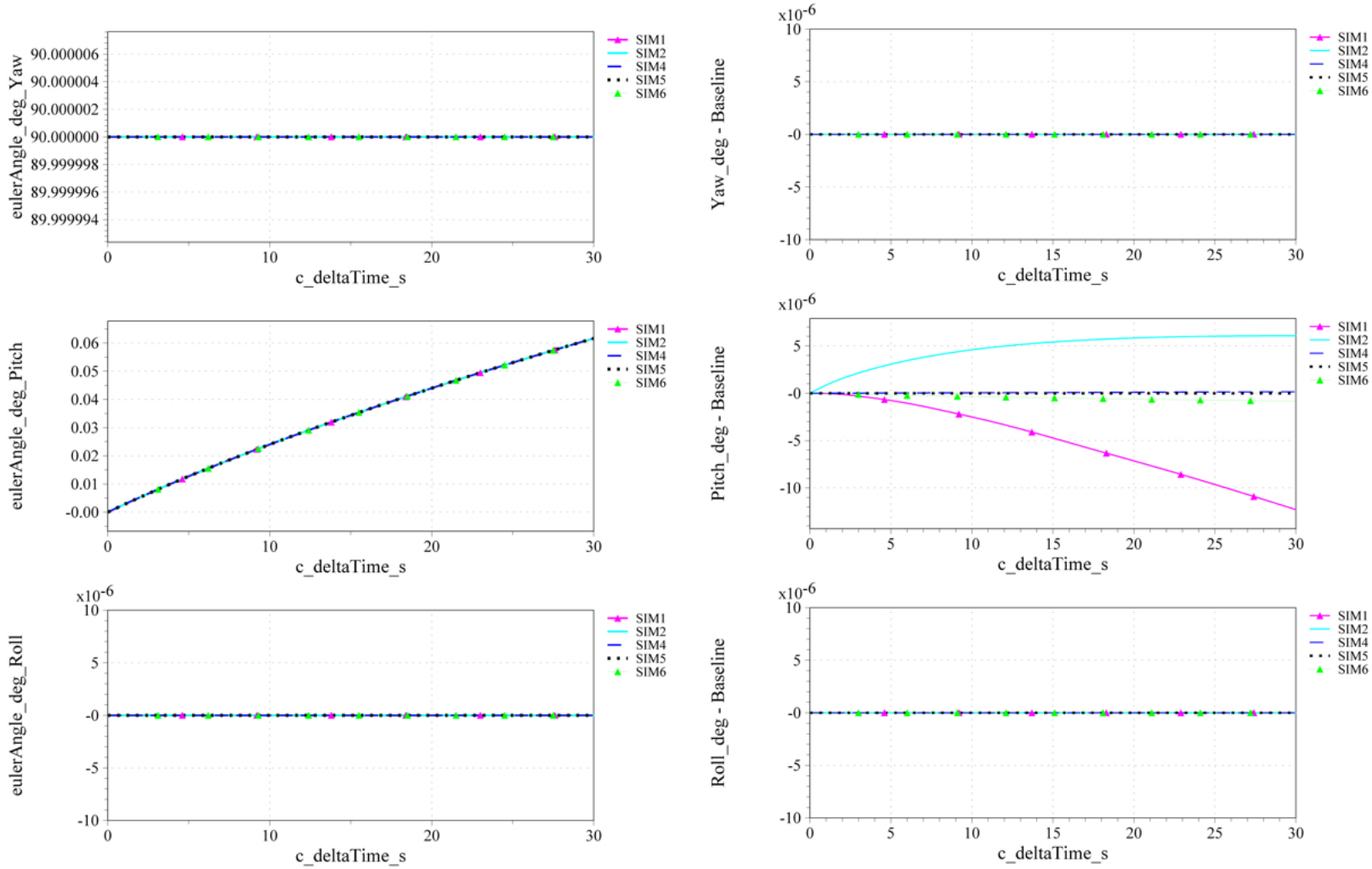

(a) Comparison of Euler Angles

(b) Differences in Euler Angles

Figure 3. Atmospheric Scenario 9 Results for Euler Angles with Respect to the North-East-Down Frame

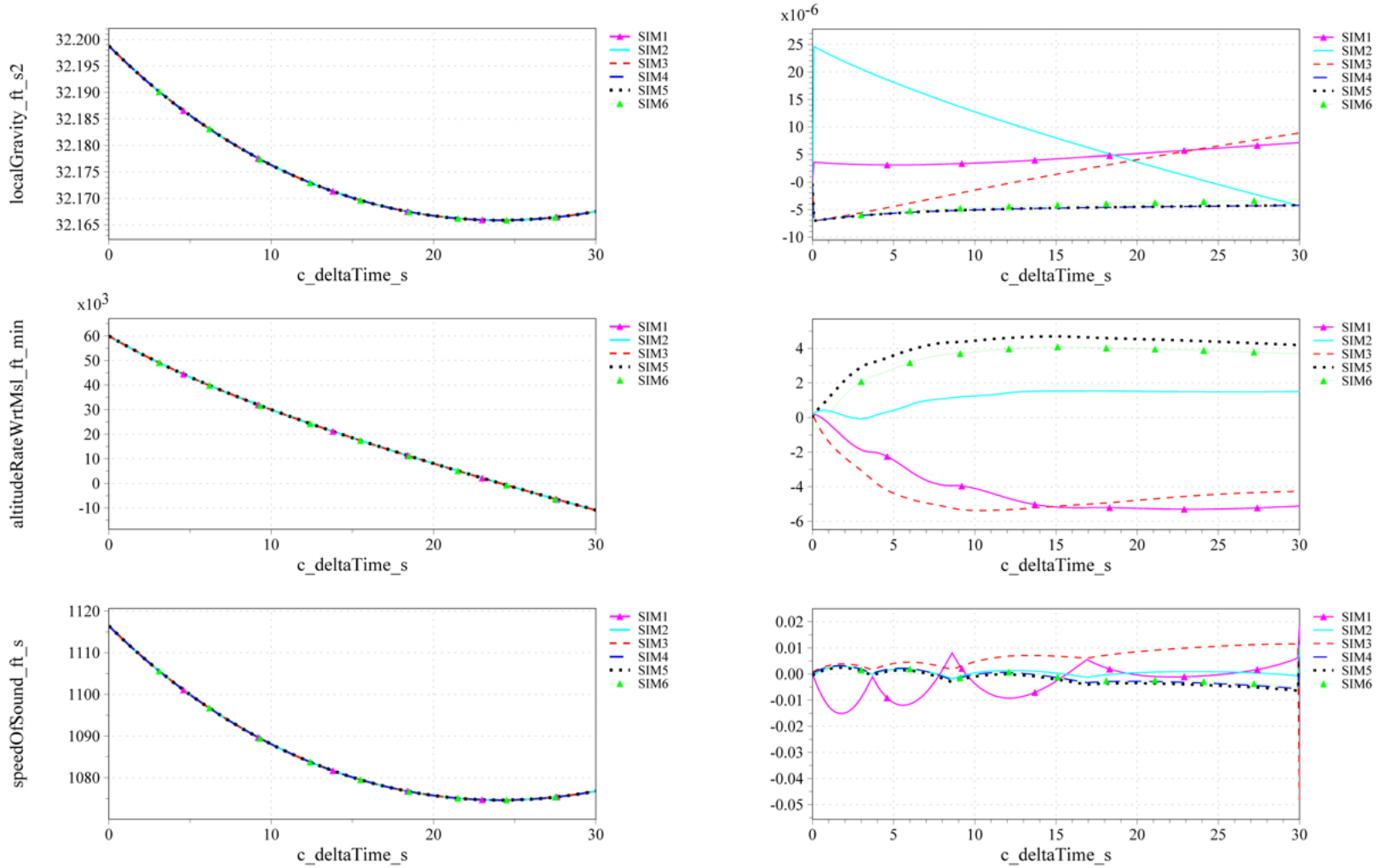

(a) Comparison of Graviation, Altitude Rate, and Speed of Sound

(b) Differences in Gravitation, Altitude Rate, and Speed of Sound

Figure 4. Atmospheric Scenario 9 Results for Gravitation, Altitude Rate, and Speed of Sound

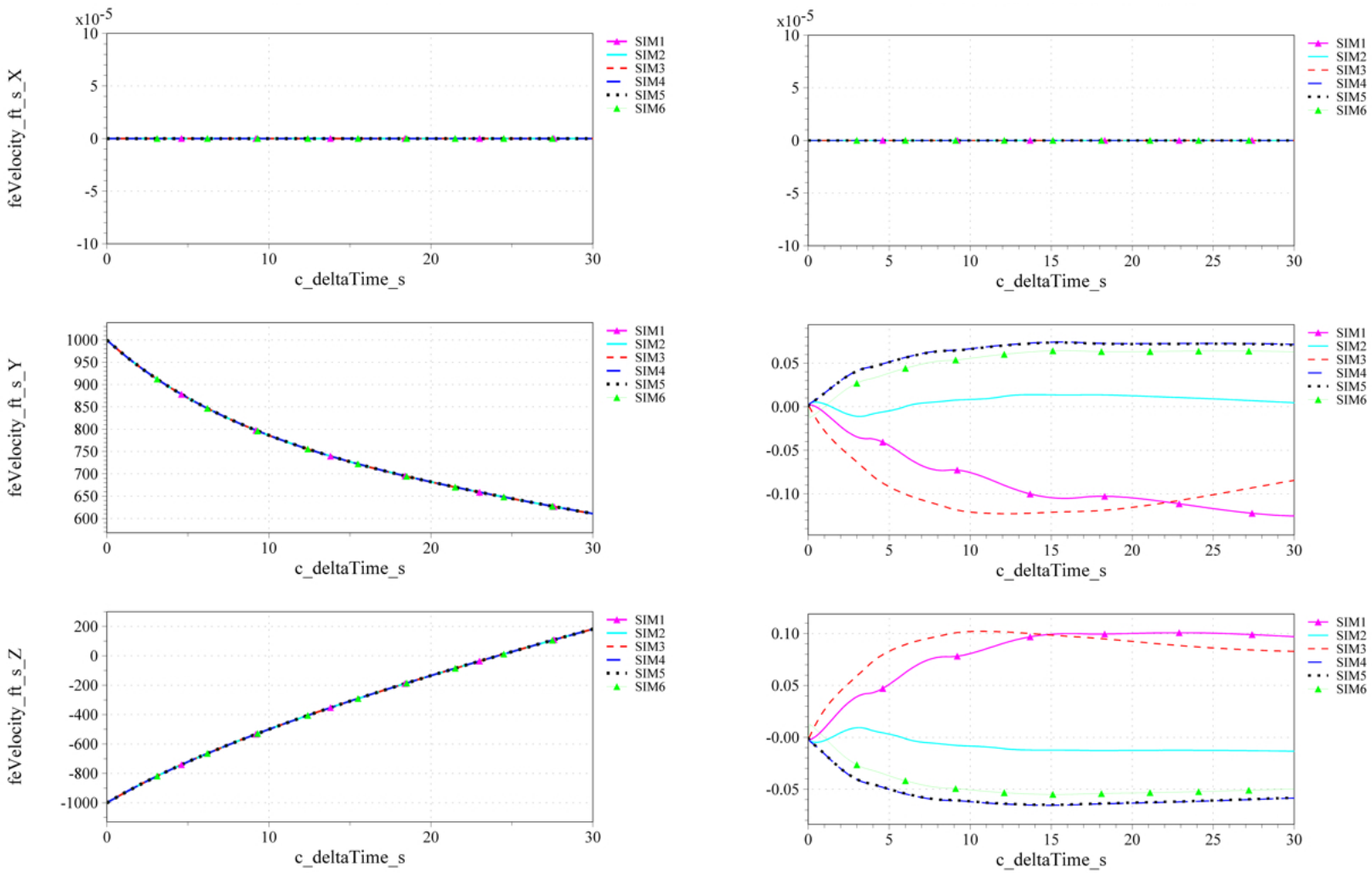

(a) Comparison of North-East-Down Velocity

(b) Differences in North-East-Down Velocity

Figure 5. Atmospheric Scenario 9 Results for North-East-Down Velocity

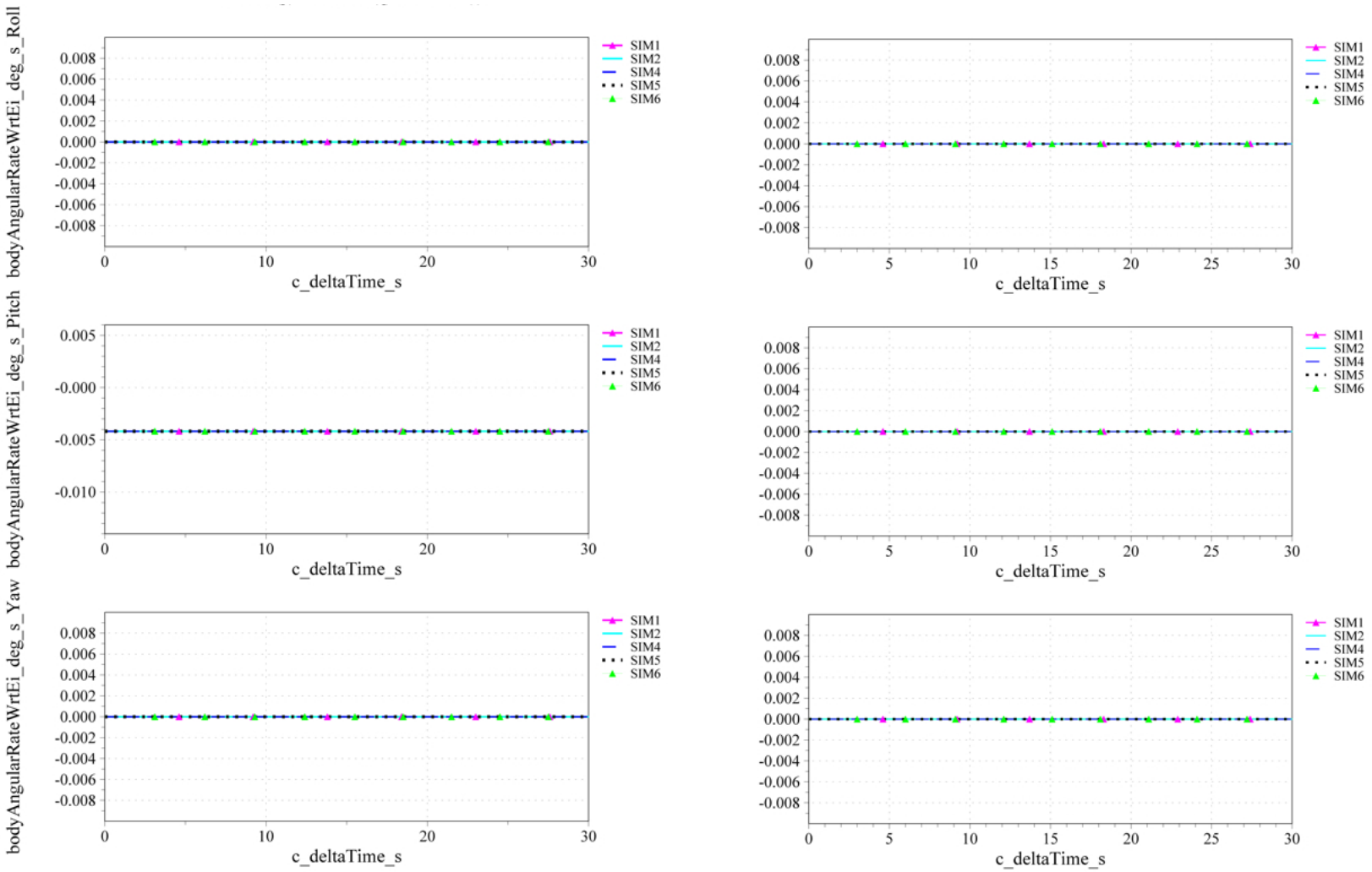

(a) Comparison of Inertial Angular Rate in Body Axes

(b) Differences in Inertial Angular Rate in Body Axes

Figure 6. Atmospheric Scenario 9 Results for Inertial Angular Rate in Body Coordinates

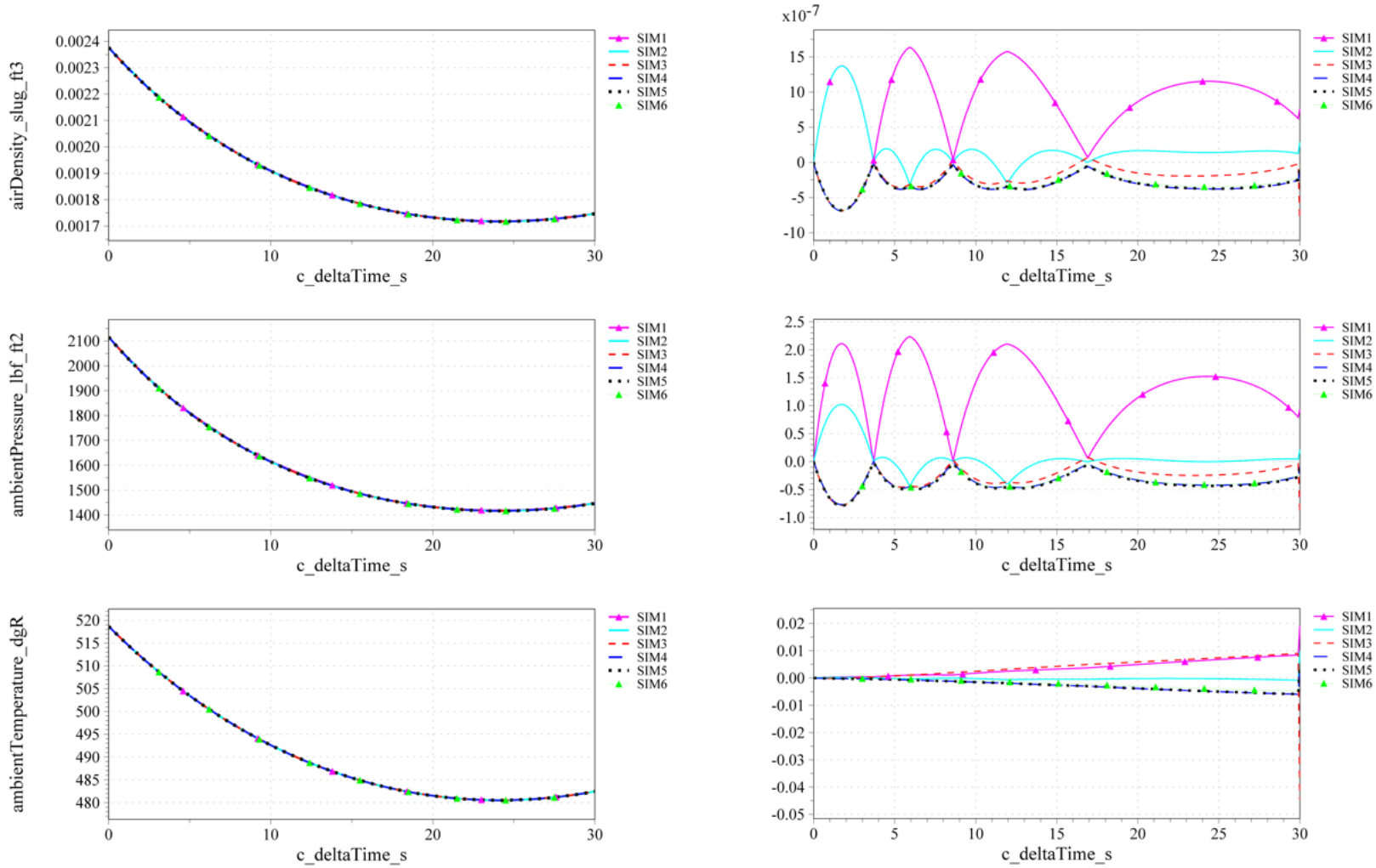

(a) Comparison of Atmospheric Properties

(b) Differences in Atmospheric Properties

Figure 7. Atmospheric Scenario 9 Results for Atmospheric Properties

2. F-16 Check Case

This selected scenario utilized the F-16 model. The vehicle was to be uncontrolled, as this was a test of how well the vehicle was trimmed for straight and level flight for non-trivial initial conditions (given in Table 5): positioned 10,000 ft above First Flight airport in Kitty Hawk, NC on a heading of 45° true at 400 kt true airspeed (KTAS) relative to the still atmosphere.

Each simulation's trim solver solved for zero linear and angular accelerations (1 g flight) at 400 KTAS at 10,013 ft MSL by varying pitch attitude, elevator position, and throttle setting.

Table 5. Initial conditions for atmospheric scenario 11.

Scenario	11: Subsonic winged flight (trimmed straight & level)			
Vehicle	Unaugmented F-16			
Geodesy	WGS-84 rotating			
Atmosphere	US 1976 STD; no wind			
Gravitation	*J2*		**Duration**	180 s
Initial states	**Position** (deg, deg, ft msl)	**Velocity** ft/s	**Attitude** deg	**Rate** deg/s
Geodetic Local-relative Body axes	[36.01916667, -75.67444444, 10013]	[400, 400, 0]	[0, 0, 45]	[0, 0, 0]
Notes	Initial position is 10,000 ft above KFFA airport (13' MSL) on a 45° true course. True airspeed 335.15 knots. Stability augmentation off. Test of trim solution.			

This check-case was the first of a series utilizing the F-16 model. Unlike the first ten atmospheric scenarios, the F-16 scenarios required that the simulation tool generate an equilibrium ("trim") solution for the F- 16 vehicle model so that its initial state, including control surface deflections and engine thrust, resulted in straight and level flight. This equilibrium solution requirement can introduce differences among the simulation implementations since different simulation tools may have different definitions for straight and level flight, especially over the curved surface of a round or ellipsoidal Earth. Simulation tools may also generate solutions with different tolerances for residual acceleration.

Such differences can be seen in Figure 8 through Figure 13 for the three simulations that provided data for this check-case. All three simulations used slightly different assumptions about the angular rate necessary for straight and level flight (Figure 13). SIM 2 constrained the angular rate to be zero in the inertial frame. SIM 4 solved for the pitch rate that maintained the pitch angle as the vehicle flew over the curved surface of the Earth. SIM 5 solved for the three-axis angular rate that maintained the vehicle orientation (i.e. all three Euler angles) relative to the local vertical frame as the vehicle flew over the curved surface of the Earth. Even so, the equilibrium roll and yaw rate computed by SIM 5 were very small, 3×10^{-5} and 8×10^{-4} deg/s respectively. Therefore, the equilibrium solutions for SIM 4 and SIM 5 were nearly identical. Nevertheless, each simulation exhibited an oscillation in angular rates during the first second of the simulation. Differences during the oscillation dwarfed the initial attitude differences. Once the oscillation settled, however, SIM 4 and SIM 5 were in near agreement on angular rate while the trajectory calculated by SIM 2 continued to differ from SIM 4/5.

The initial roll and pitch angle in SIM 2 also differed from SIM 4/5 (Figure 11). The root cause was a difference in the simulated gravity vector. SIM 2 employed a simplification that creates a gravity vector that is slightly deflected from the surface normal. (Here, the terms gravitation and gravity have different meanings: gravitation is the force from the attraction of two masses; gravity is the sum of gravitation and the centrifugal acceleration due to the Earth's rotation. Gravity is the acceleration of a body in free fall measured by an observer stationed on the surface of the Earth.) All three simulations computed the geocentric gradient of the J_2 gravitation potential, which produced gravitation in the geocentric down direction and a much smaller contribution in the geocentric north direction. However, SIM 2 approximated the geodetic NED frame using the geocentric frame as the local vertical local horizontal (LVLH) frame when computing gravity. SIM 4 and SIM 5 translated the geocentric gravitation vector into a geodetic gravitation vector. This rotation was necessary to produce a gravitation vector where the

resulting small geodetic north-axis component of gravitation was canceled by the geodetic north-axis contribution of centrifugal acceleration due to the Earth's rotation. This resulted in a gravity vector whose direction matched the geodetic down-axis direction almost exactly. Without rotation to the geodetic frame, the gravitation and centrifugal acceleration combined to create a gravity vector slightly deflected from the geocentric downward direction. That deflection was equal to the difference between the geodetic and geocentric latitude since the true direction of the gravity vector is along the geodetic normal.

In the initial position specified by this check-case, the resulting gravity vector, in geocentric coordinates, is deflected 0.18 degrees southward of the radial vector. That deflection amount was approximately equal to the difference in roll angle between SIM 2 and SIM 4/5. The equilibrium solver for SIM 2 appeared to roll the vehicle slightly so that its aerodynamic lift was more closely aligned with the slightly non-vertical gravity vector. The SIM 2 equilibrium solver also produced a slightly different pitch angle because the aerodynamic lift required for the trim solution differed slightly from those of SIM 4/5. With a non-zero roll angle, eliminating vertical acceleration in SIM 2 required balancing contributions from weight, thrust, lift, drag, and aerodynamic side force. When the roll angle was zero, as in SIM 4 and 5, no significant aerodynamic side force was generated.

Even if SIM 2 were modified to use a geodetic gravity vector, the difference plot for gravitation (Figure 12) shows that there would remain a small difference in gravitation of 1.8×10^{-4} ft/s^2. There should be no difference in Earth parameters among the simulations given that the simulations match J2 gravitation for atmospheric case 1 as described in Ref. 9. What remains as a possible explanation of this difference in gravitation could be a difference in the conversion from the initial geodetic coordinates to an initial geocentric position. The difference could be significant. For example, a reduction of 58 feet in the geocentric distance of the vehicle would produce the same change in magnitude. Nevertheless, the difference in magnitude should be a minor contributor to the vehicle dynamics as it adds only 0.11 lbf to the weight of the 20,500 lb F-16 example vehicle.

Differences in initial angular rates would induce differences in the aerodynamic forces and moments. However, those differences were very small and were dwarfed by other contributors including the contribution from the angular rate oscillation in the first second of the simulation (Figure 13).

A substantial difference in the plotted aerodynamic moments (Figure 9) is the result of a difference in the reference location for recording aerodynamic moments. When recording the aerodynamic moments, SIM 2 recorded moments about the aerodynamic moment reference center (MRC); SIM 4 and 5 recorded the aerodynamic moment at the vehicle center of mass (CM) after these had been transferred from the MRC. This difference appears in the aerodynamic moment plots for all the F-16 cases; it just reflects a lack of agreement on which moment vector to record.

Even when the moments were adjusted for differences in the reference point, a difference in the initial aerodynamic yaw and pitching moments remained between SIM 2 and SIM 4/5 at the MRC; furthermore, SIM 2 also differed in the initial aerodynamic forces (Figure 8). These differences resulted from the difference in the gravity vector as described previously. With the gravity vector deflected from the local vertical in SIM 2, SIM 2 required a trade-off in pitch angle and roll angle to create the right combination of angle of attack and sideslip such that the resulting aerodynamic lift and side-force counteracted the gravity vector while leaving no residual force in the horizontal plane. As discussed above, the result is a roll angle that nearly aligned the body z-axis with the deflected gravity vector. The differing lift required a different aerodynamic pitching moment to counteract the lift-induced pitching moment at the CM. The resulting aerodynamic side force also induced a yawing moment at the CM and therefore required a counteracting aerodynamic yawing moment which was not present in SIM 4 and SIM 5. That yawing moment was achieved, in SIM 2, by setting the rudder to a non-zero initial value.

The above differences, in general, set SIM 2 on a different trajectory from SIM 4 and SIM 5. After 180 seconds, the difference in vehicle positions between SIM 2 and SIM 4/5 was approximately 666 feet according to the recorded values of latitude, longitude, and altitude (Figure 10). The position difference between SIM 4 and 5 at the end of the scenario was two orders of magnitude smaller, at approximately 4 ft.

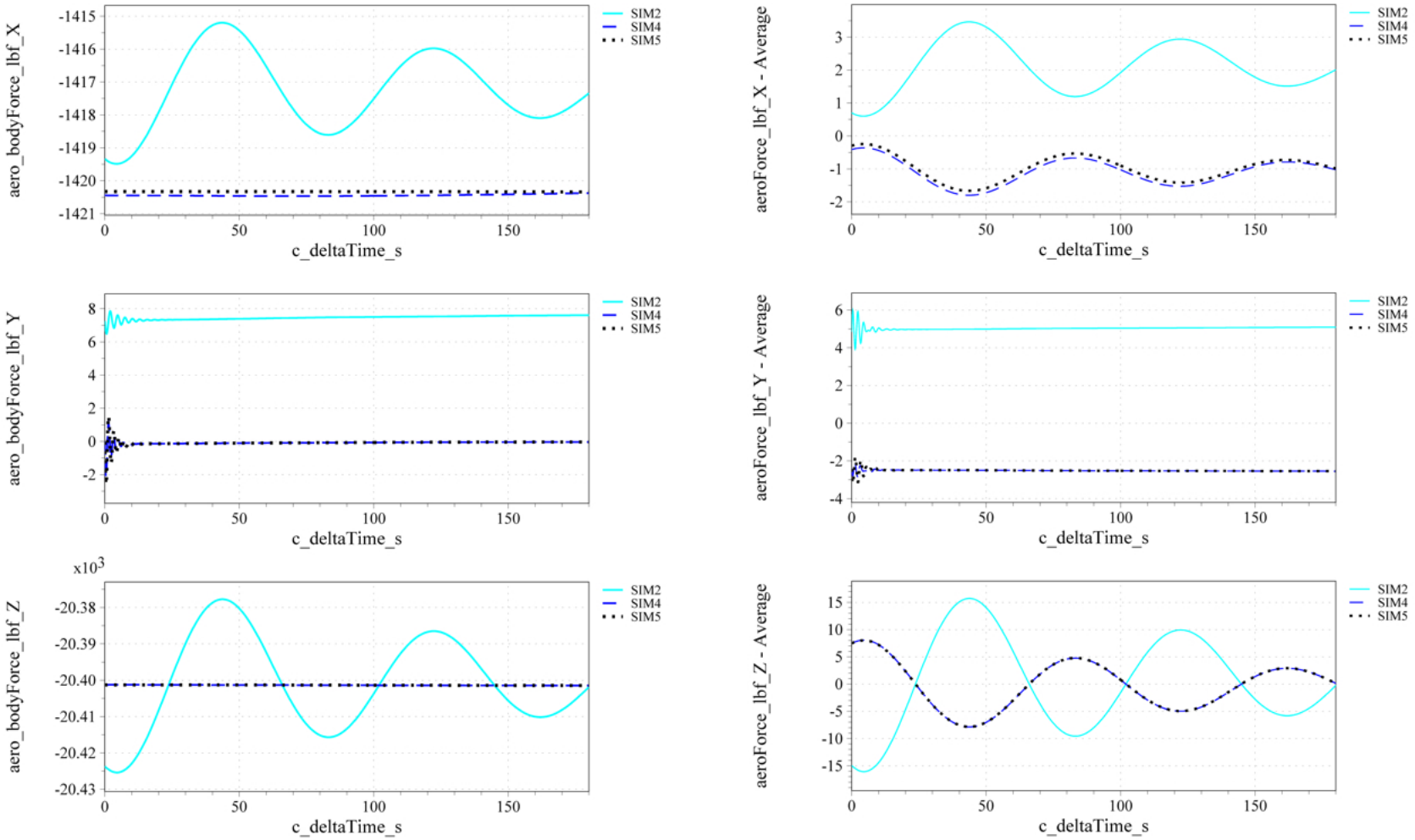

(a) Comparison of Aerodynamic Forces

(b) Aerodynamic Force Differences

Figure 8. Atmospheric Scenario 11 Results for Aerodynamic Forces

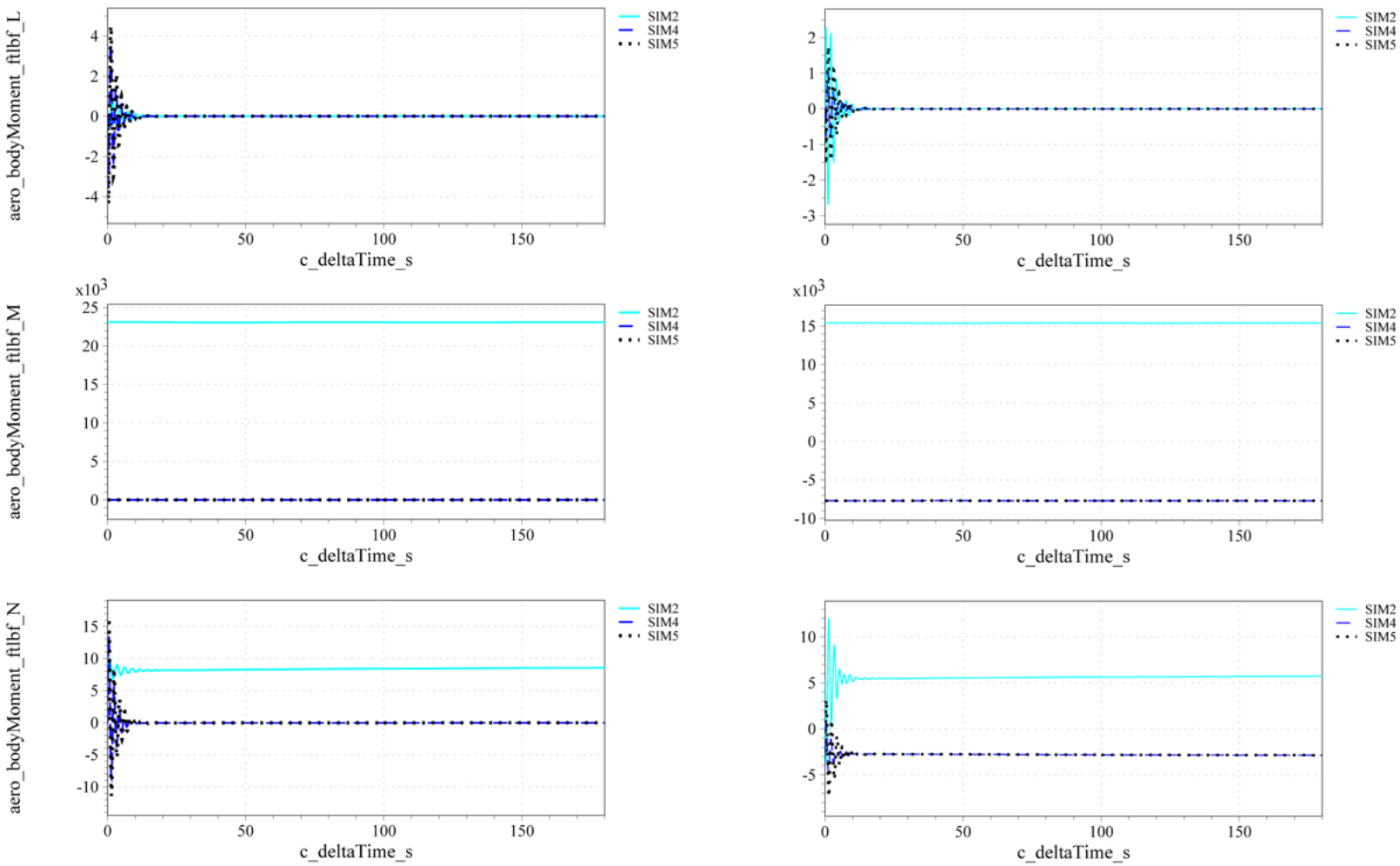

(a) Comparison of Aerodynamic Moments

(b) Aerodynamic Moment Differences

Figure 9. Atmospheric Scenario 11 Results for Aerodynamics Moments

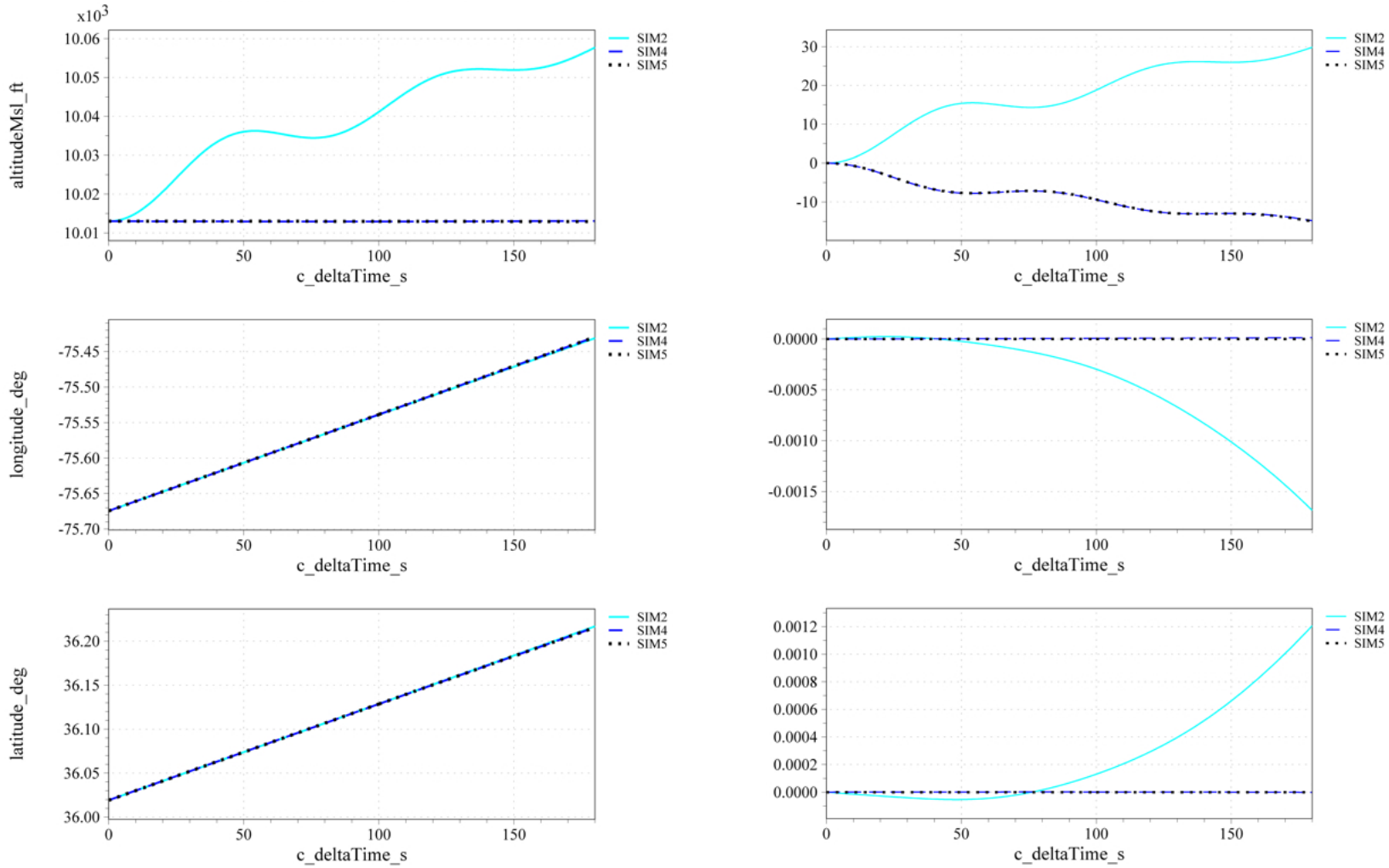

(a) Comparison of Geodetic Position

(b) Geodetic Position Differences

Figure 10. Atmospheric Scenario 11 Results for Geodetic Position

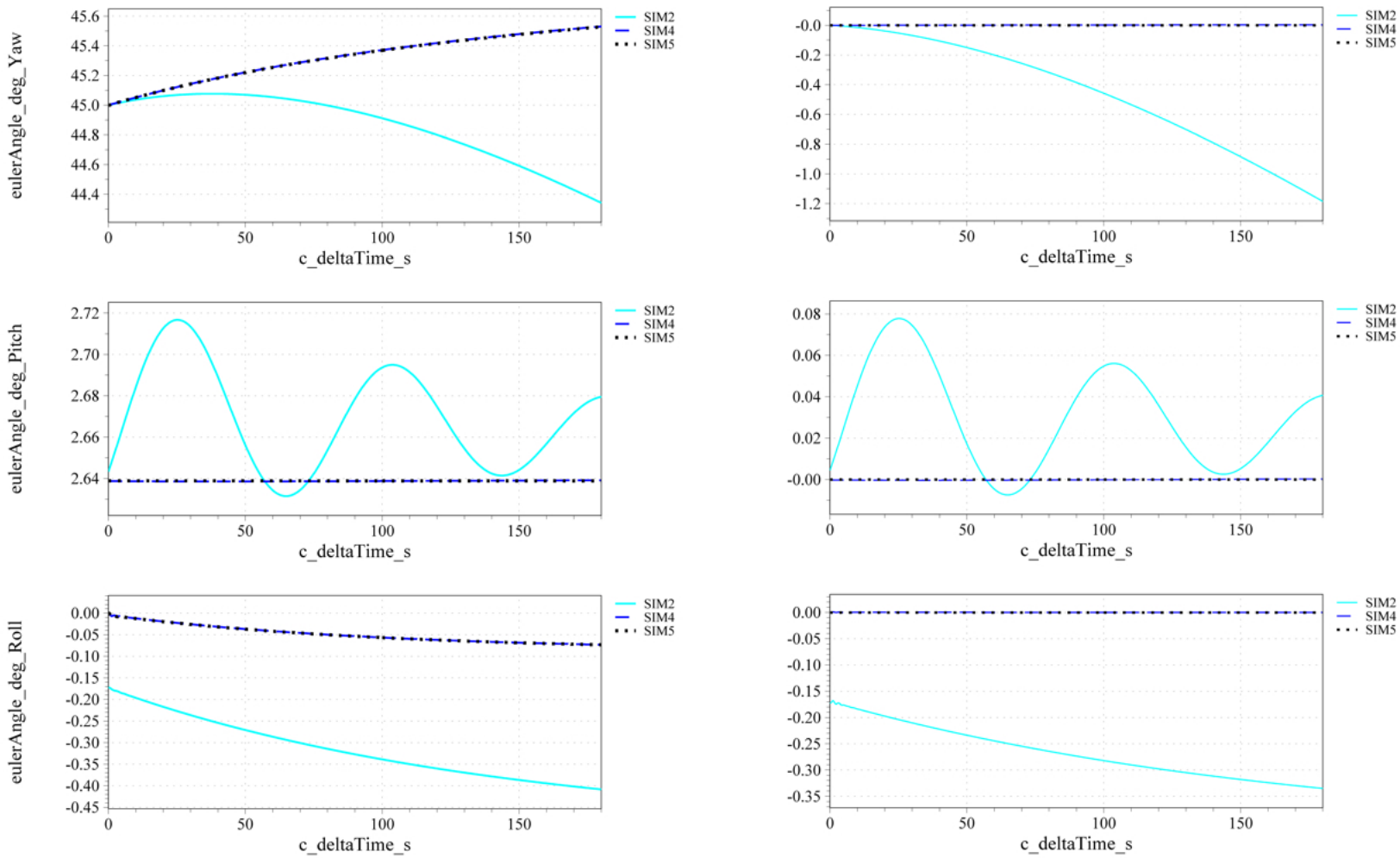

(a) Comparison of Euler Angles

(b) Euler Angle Differences

Figure 11. Atmospheric Scenario 11 Results for Euler Angle with Respect to North-East-Down Frame

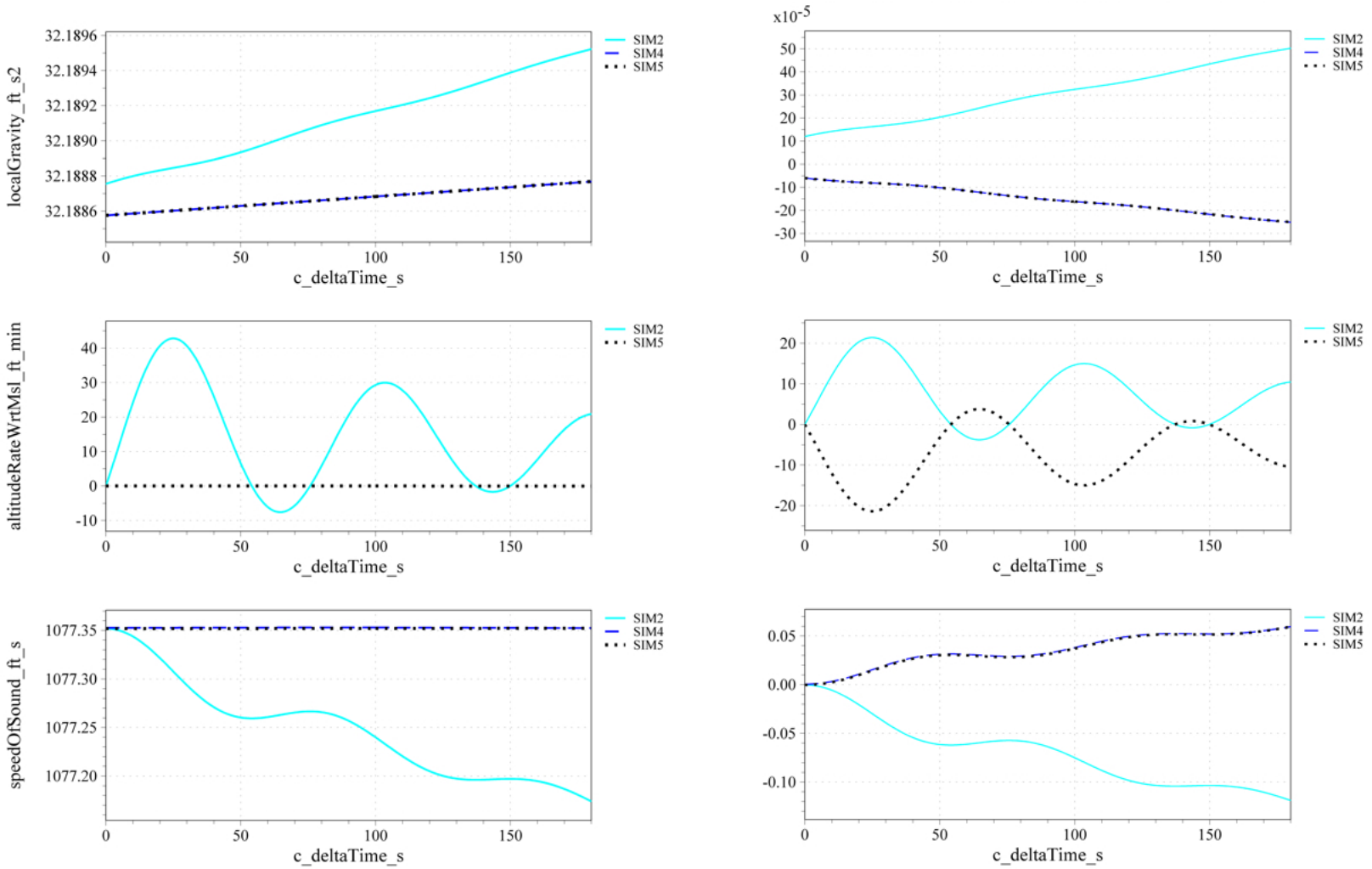

(a) Comparison of Gravitation Magnitude, Altitude Rate, and Speed of Sound (b) Differences in Gravitation Magnitude, Altitude Rate, and Speed of Sound

Figure 12. Atmospheric Scenario 11 Results for Gravitation Magnitude, Altitude Rate and Speed of Sound

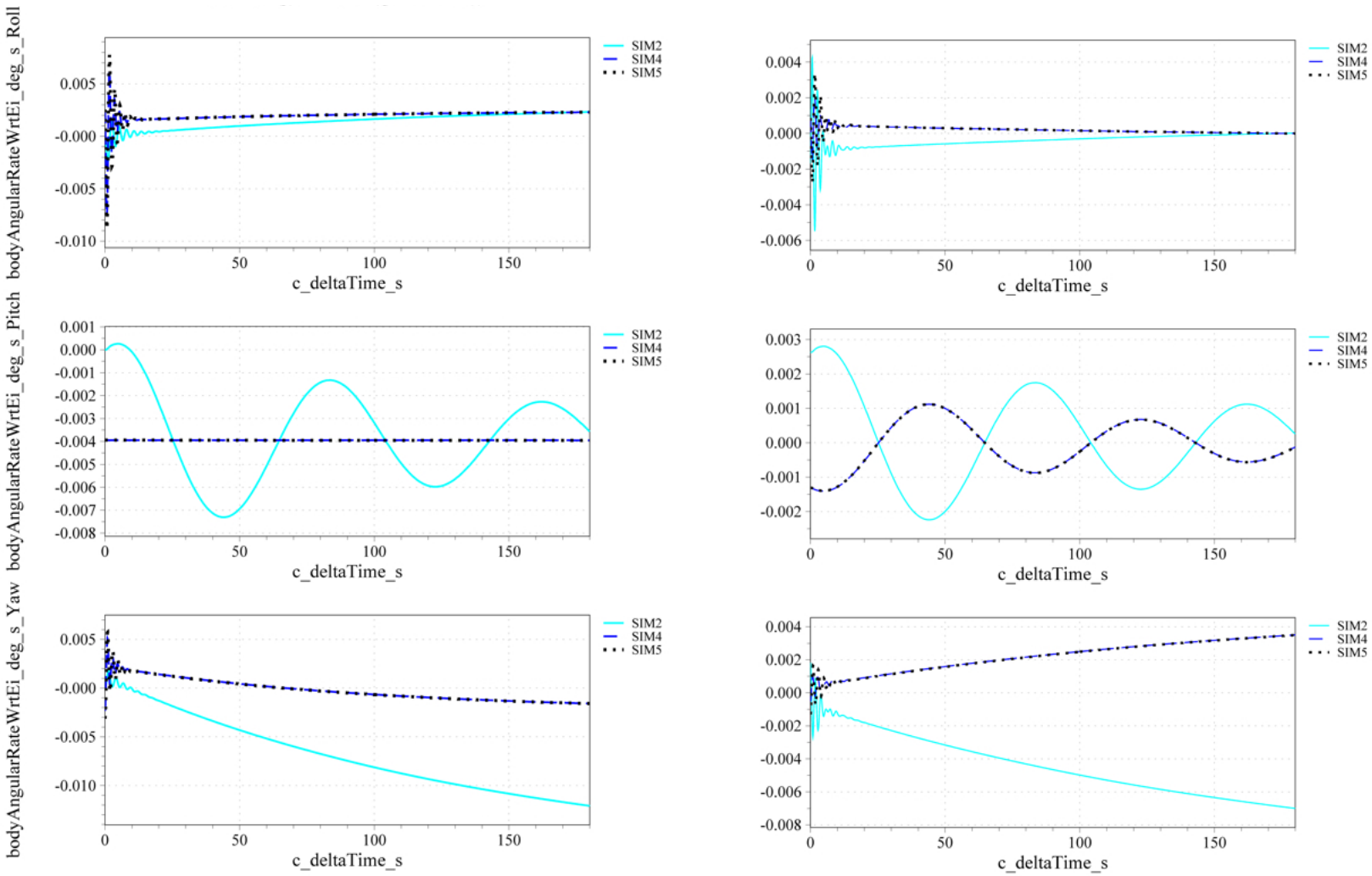

(a) Comparison of Angular Rates

(b) Angular Rate Differences

Figure 13. Atmospheric Scenario 11 Results for Inertial Angular Rate in Body Axes

B. Orbital Check-case Examples

There is less variation in the results among the simulations participating in the orbital cases. Therefore, a single case is presented to typify the outcome of the simulation comparison (all 27 check-cases are discussed in detail in reference 9 and data sets are available at the URL specified by reference 3). The selected orbital check-case is 9D which exercised both translational and rotational motion by applying both a square pulse thrust and a square pulse torque to the representative ISS mass. The detailed conditions of this check case are provided in Table 6; details on the parameters for the Earth and terrestrial time are found in Table 73 of Ref. 9. In this check case, the vehicle begins in a nearly circular orbit with an initial inertial rotation that attempts to maintain the vehicle orientation relative to the orbit. At $t = 1000$ s, this check-case applied a force of 10 N in the positive body x-axis direction through the vehicle's center of mass and a torque of 10 N-m about the positive body x-axis. The external force and torque were applied for an additional 1000 s, then were set to zero for the remainder of the run.

Table 6. Orbital Scenario 9D Description

vehicle type	ISS
orbit type	nearly circular
atmosphere model	Off
aerodynamic drag	Off
gravitational model	inverse-square
gravity gradient	Off
sun/moon gravitational perturbations	Off
Initial inertial rotation rate (body axis)	[0.000000; -0.065000; 0.000000] deg/s
Initial LVLH attitude (3-2-1 Euler sequence)	[0.000000; -11.600000; 0.000000] deg
Initial inertial position	[-4,292,653.4; 955,168.47; 5,139,356.57] m
Initial inertial velocity	[109.649663; -7,527.726490; 1,484.521489] m/s
Start Time (UTC)	2007/324:00:00:00

Select results are provided in Figure 14 through Figure 16. One challenge that this check case presented to a simulation is the modeling of the force and torque as a square pulse. The integration error of a numerical integration technique can increase substantially as it encounters the discontinuous leading and trailing edges of the square pulse. Furthermore, a one-frame lead or lag in the start or end of the square pulse causes a substantial difference in the results that follow. Some early iterations in the comparison were spent establishing and confirming the exact timing of the leading and trailing edge of the square pulses among the simulations.

Figure 14 shows the predicted orbit-relative attitude of the vehicle presented as LVLH Euler Angles. SIM B and SIM C agreed on the vehicle attitude; differences between them were negligible. Compared to SIM B and C, SIM D exhibited a minute difference in angular momentum at the leading edge of the torque pulse (as evidenced by the inertial angular rates in Figure 15) but remained steady after the trailing edge of the input. The amplitude and duration of the difference in angular momentum caused the momentary spike in difference for LVLH Euler angles, but the long-term increase in difference was very modest. Moreover, these differences were considered insignificant. SIM A shows a minute difference in angular momentum, relative to the other simulations, after completing the torque pulse (see the angular rate differences in Figure 15). The difference in angular moment is likely caused by a difference in integration method. This minute difference in angular momentum caused the increasing difference in the LVLH Euler angles over time. As detailed in Ref. 9, results for prior orbital check-case 8B reveal that, under torque-free rotation, differences in integration methods among the simulations contribute to differences in Euler Angles of order up to 10^{-5} radians, and those differences would also manifest here. Nevertheless, the overall differences in attitude for this case were not significant.

Differences in rotational rates between the simulations were negligible and were attributed to differences in integration method as explained in the previous paragraph or differences in the precision of the recorded data. The one exception was the difference in the initial inertial pitch rate for SIM D (see Figure 15). Although hard to see in the plots, SIM D recorded a sudden jump in pitch rate from 0 rad/s at $t = 0$ to 0.0011 rad/s at $t = 60$ s (the next recorded frame). However, this jump appeared to be an artifact of the data recording as the Euler angles showed no response to this jump. Nevertheless, this jump was sufficiently large to require the comparison plots to use a range that was too large to display the differences between the simulations in the rest of the maneuver. Even so, those differences were similar in magnitude to the differences seen in the roll and yaw rates.

For SIM B, SIM C, and SIM D, those rotational state differences did not contribute significantly to the differences in translational state, as a result of influencing the direction of the thrust vector. The differences in translational state among these simulations were negligible as evidenced by the inertial position differences in Figure 16. SIM A, however, exhibited Euler angle differences due to integration residuals that caused the inertial position to depart slightly from the other solutions. The inertial position difference grew to less than 2 meters at the end of the simulated eight hour flight. However, the differences are entirely attributed to the combined integration residuals for both the rotational and translational motion, and not to any differences in modeling or equations of motion. Thus, whether it was SIM A or the other three simulations exhibiting increased integration residue, the integrators could likely be reconfigured to reduce the difference in position if an application required greater accuracy in results.

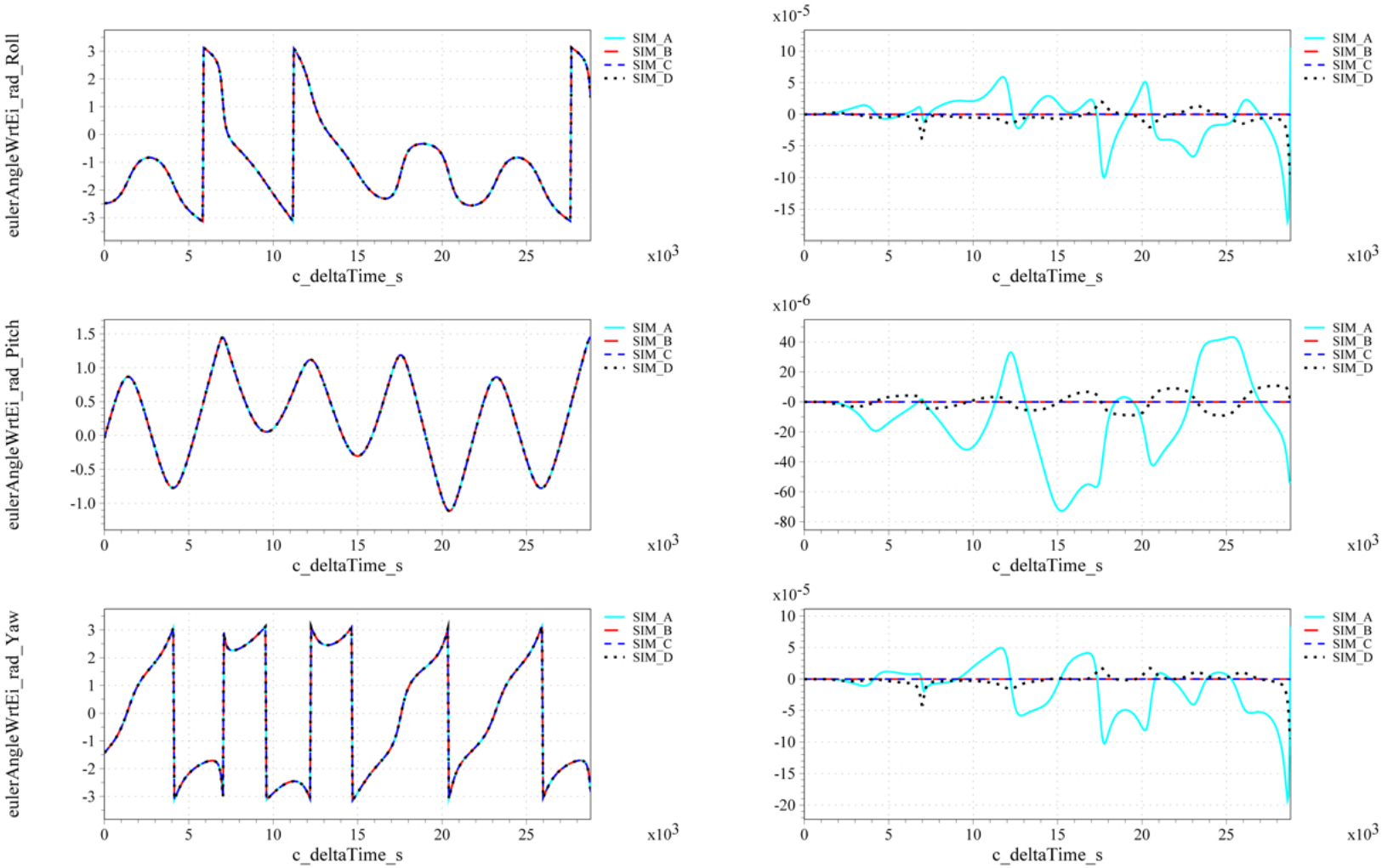

(a) Inertial Euler Angles Compared

(b) Inertial Euler Angles Differenced

Figure 14. Inertial Euler Angle Results for Orbital Scenario 9D

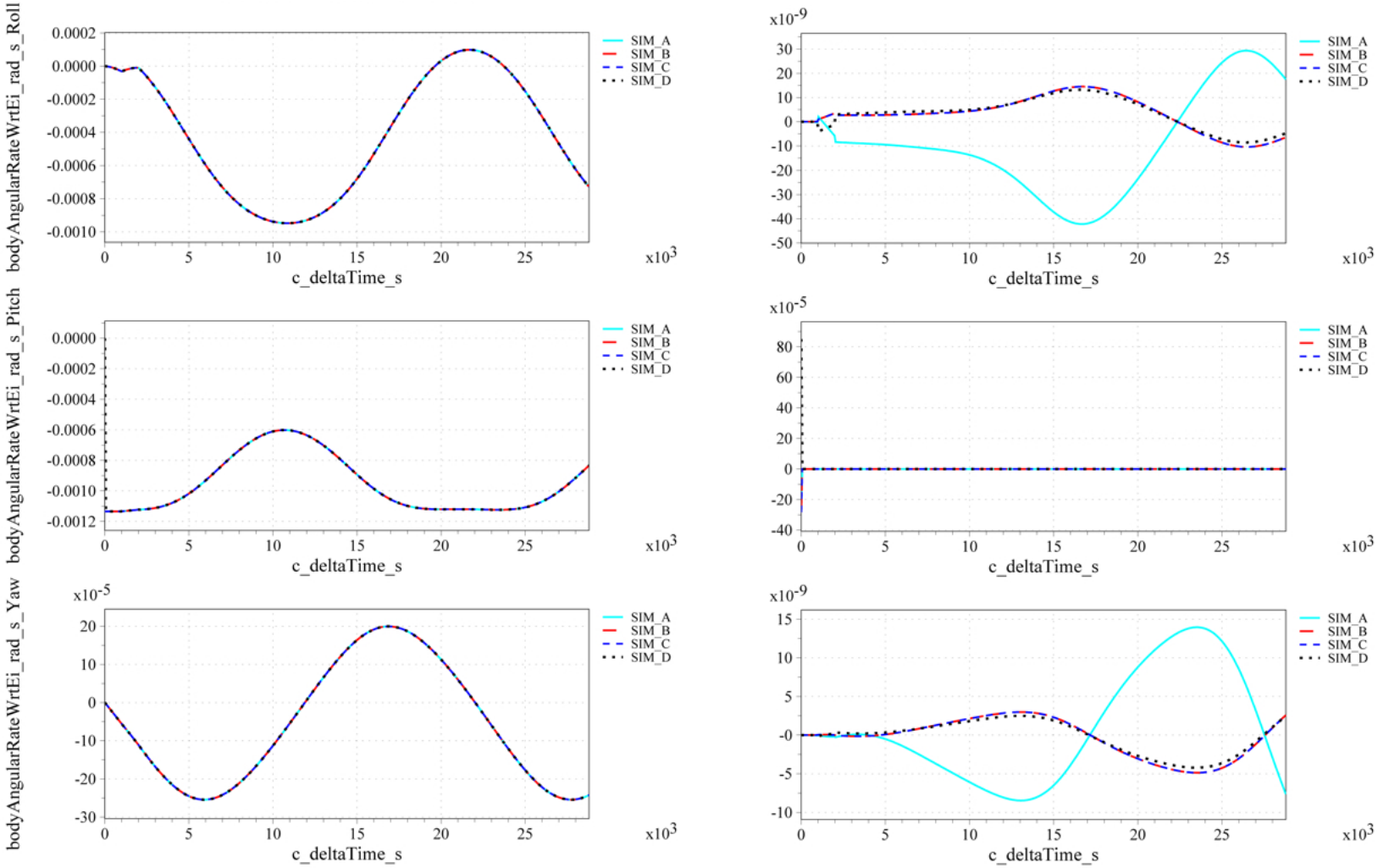

(a) Inertial Angular Rates Compared

(b) Inertial Angular Rates Differenced

Figure 15 Orbital Scenario 9D Results for Inertial Angular Rate in Body Coordinates

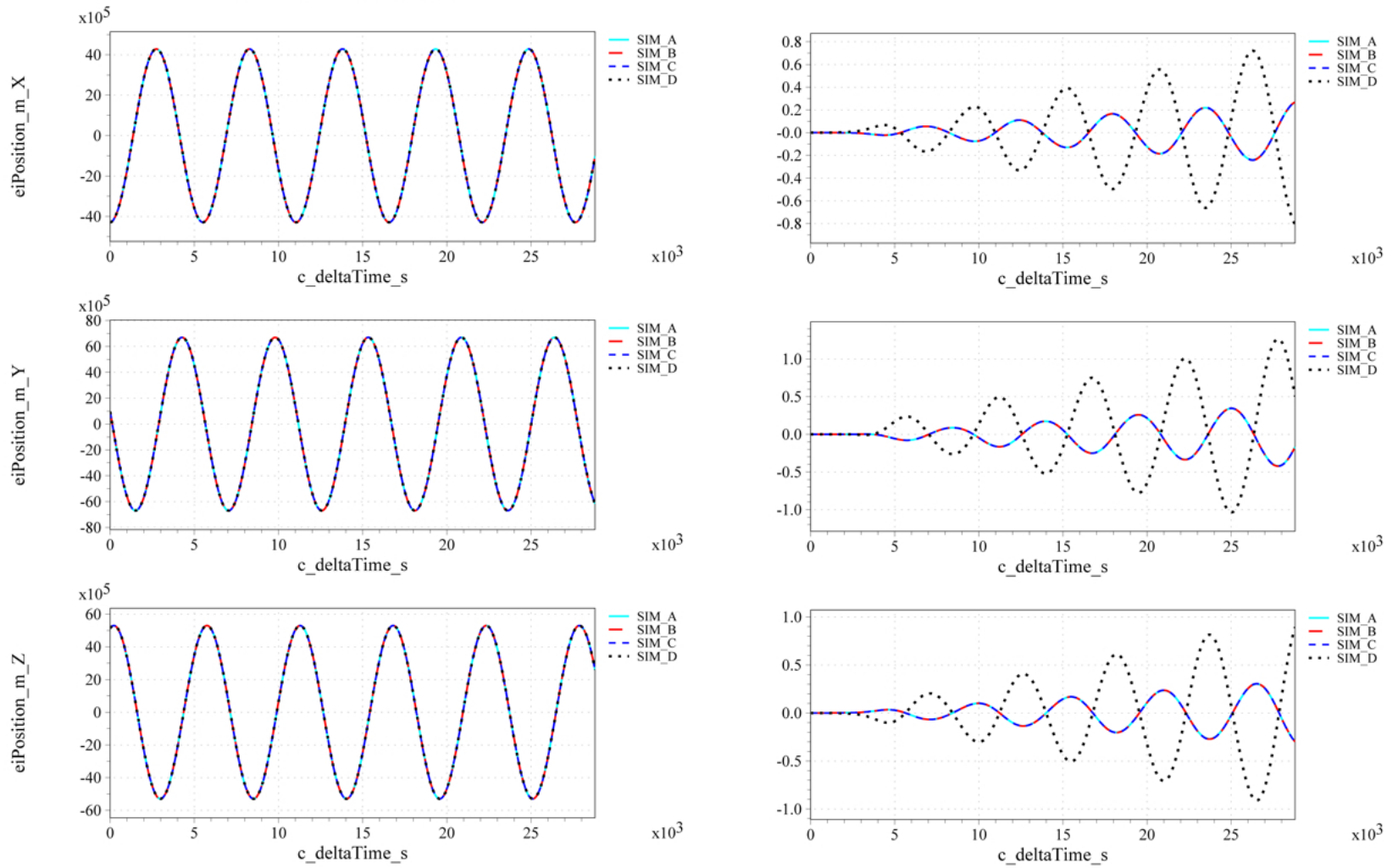

(a) Inertial Position Compared

(b) Inertial Position Differenced

Figure 16. Orbital Scenario 9D Results for Inertial Position

IV. Summarized Results

A ground rule used by the team in providing comparisons was that at least three simulation tools had to submit results for each check-case before it could be analyzed. Additional planned cases (e.g., supersonic fighter maneuvering flight and a proposed Apollo-like capsule reentry) were not included due to an insufficient number of implementations achieved. A total of 16 of the 17 atmospheric check cases were completed and all of the 27 orbit check cases were completed.

A. Atmospheric check-case results

In general, comparisons of the atmospheric check-cases as simulated by several simulation tools indicate minor differences due to two variations in implementation: tabular versus equation-based atmosphere models, and geodetic versus geocentric geometries.

In earlier computationally-constrained simulation implementations, an atmosphere model (e.g., Ref. 7 employed for these atmospheric flight simulations) was implemented as a table of density, temperature, and pressure values as a function of geometric height above a reference surface. This table was used in a linear interpolation between altitudes since this was typically faster than performing the complex calculations necessary to determine these quantities algebraically. Improved processors have made the direct calculation approach economically feasible and more precise. However, several of the participating simulation tools continue to use an atmospheric table implementation. Therefore, some of the trajectory differences are due to linear interpolation of atmospheric properties.

The other main difference between results in atmospheric comparisons is an artifact of historical simulation techniques. As mentioned, early digital flight simulations of subsonic aircraft often assumed a flat Earth, where latitude and longitude were directly related to a Cartesian grid in the vicinity of a runway or airport. This was an appropriate approximation for low-speed flight in the vicinity of and while maneuvering around the terminal environment. Since the check-cases specified at least a round Earth, some retrofitting was undertaken to adapt the flat-Earth approximations in some participants to a round or oblate Earth. However, some artifacts of the simpler geodesy assumption remain which affect geodetic coordinate calculations and the direction of gravity relative to the local vertical.

To a smaller degree, some variances in the implementation of the square-law and harmonic gravitation were due to differences in gravitation model implementation, or in the conversion of the initial geodetic position into the geocentric position. Another variance source in the F-16 check-cases was differences in defining the equilibrium (i.e., trim) values for straight and level flight, especially the trimmed rotational rate.

Errors in participating simulation tools that were initially uncovered, and corrected, included mistakes in gravitational models, incorrect or imprecise initial condition values and geophysical constants, a one-frame time shift in gravitational value, and a transposition error in atmospheric property tables. For example, one simulation routinely and incorrectly aligned gravitational attraction along the geocentric radius axis, not the geodetic nadir. This led to a very, very small difference in the resulting trajectories that might not have been quickly identified without this exercise.

Finally, differences in numerical integration methods in the simulation tools appeared to cause trajectory differences. These differences are hypothesized, as no specification of (or sufficient data regarding) integration techniques was initially available.

In all cases, these differences were minor. Most were only visible when plotting variances between individual simulation results versus consensus or averaged results.

It should be noted that obtaining correlation between these simulations was an iterative process. Initial results were not as good as those ultimately obtained due to ambiguity in specification or implementation of initial conditions, maneuver inputs, and other simulation implementation differences.

A total of 84 trajectories were generated, comprised of nearly four million data points; these data sets are stored in 64 MB of data files available in the data repository[3].

B. Orbital Check-Case Results

Comparison of orbital check-cases showed good comparisons with few significant differences. As with the atmospheric cases, some iteration was required as significantly different results were initially obtained. These differences included use of different revisions of the MET model, differences in the specification of the Earth's

position at the start of various scenarios, differences in integration technique, or to misinterpreting a sign convention or initial condition specification.

An error was discovered (and corrected) in one of participating simulation tools in which an external force or moment was applied for a length of time other than what was specified in the configuration. This error was introduced in a recent rewrite of that particular module of the simulation tool and had somehow managed to elude detection, despite extensive regression tests that are routinely applied to all revisions. The revised tool had not yet been released, but the error may have affected NASA missions if it had not been detected during this exercise. The tool architect stated that he believed this 'catch', by itself, justified the cost of the exercise.

A total of 103 trajectories were generated and comprise nearly 1.4 million data points. These data sets are stored in 25 MB of data files available in the data repository[3].

C. Comparison Difficulties

During this exercise, it became apparent that the time required to reach a reasonable level of match had been underestimated. The original schedule developed and agreed to by the team reflected the expectation to complete this effort in just over 12 months. The effort took 30 months and was not completed to the degree expected at the outset, in that one atmospheric check-case (Earth reentry from a lunar return trajectory) has not been attempted, and a second atmospheric case remains incomplete.

Part of the delay was due to the now-apparent need to specify initial conditions and maneuvering inputs exactly. It was believed early in the planning process that it would be sufficient for the scenarios to be described briefly in one axis frame; however, obtaining good matches ultimately required detailed specification of the initial conditions in several axis frames. An example is the initial rotation rate for some of the early atmospheric check-cases: a small numeric difference exists between the inertial and the ECEF angular rate of a body. Ensuring close matches required giving the rotation rate in both frames to ensure all simulation tools started with the same rate, since some simulation tools are initialized in ECEF-relative rates and others in inertial rates.

As knowledge was gained in this process, the initial conditions document had to be revised several times, initially leading to confusion by the team as to which version was to be used in each round of comparison plots, which delayed reaching successful matches.

The process followed by the geographically dispersed team also introduced delays. Due to the large amount of data involved, considerable time was spent uploading data sets from each tool to a central server, downloading and plotting the trajectories by one analyst, uploading the results, and downloading and inspecting the large number of resulting plots for differences. Obvious differences were fairly easy to detect, but determining the root cause of the difference often took considerable time and effort.

A formal comparison by one analyst required a period of several weeks, due to the large number of maneuvers to compare and the in-depth analysis required.

Since most participants were not assigned full-time on this exercise, some of these comparison cycles took longer than others due to NASA priorities. Many more comparison cycles were also required than originally expected (30 sets of comparison plots were generated for the atmospheric cases between May 2013 and August 2014).

V. Conclusion

The eventual matches between simulation tools, achieved only after several iterations of comparing results and correcting mistaken assumptions and other errors, were good enough to indicate agreement between a majority of simulation tools for all cases published. Most of the remaining differences are explained and could be reduced with further effort.

Simulations from atmospheric check cases found the following:

- Minor differences in results from tabular versus equation-based atmosphere models, and geodetic versus geocentric geometries;
- To a smaller degree, some differences in the implementation of the square-law and harmonic gravitation are also apparent due to differences in gravitation model implementation or in the conversion of the initial geodetic position into the geocentric position (since position is an input into the gravitation model);
- Due to differences in trim algorithms, some of the 6-DOF aircraft check-cases (cases 10-16) leave some remaining disagreements on precise numbers, but do indicate a family of solutions that are close enough to serve as a comparison with other simulation tools; and
- Differences in numerical integration methods in the different simulation tools appeared to cause some differences in predicted trajectories.

Comparison of simulations from the orbital check cases showed good agreement. The remaining differences are attributed to either an obvious misconfiguration of the simulation tool or differences in the numerical integration method and step size.

Lessons learned in this exercise include the following observations and recommendations for improving cross-simulation comparisons:

1. Modeling even simple vehicles posed challenges. Differences in the implementation of simple vehicle models were apparent. These arose primarily from differences in interpretation of the scenario and initial conditions. Initial attempts to model these scenarios led to some significant miscompares that revealed differences in physical constants and other modeling errors. These differences in constants and modeling errors were corrected in several tools with each comparison iteration.
2. It took significant effort to get good agreement on the check-cases. Even simple aerospace vehicle simulation models are non-trivial to implement. The comparable results shown in most of these check-cases required extensive iterations and adjustments/corrections to initial conditions and modeling assumptions.
3. Tabular versus equation-based atmosphere models introduced trajectory differences.
4. Different interpretations of nadir direction can lead to differences due to "non-vertical" gravitational residue.
5. While the majority of atmospheric simulations appeared to use WGS-84 Earth geodesy, simplifications in simulations originally designed for flat-Earth or round-Earth led to trajectory differences. Therefore, Flat-Earth or round-Earth simplifications should only be used when appropriate.
6. Precise specification of initial conditions would be assisted by a standard for specifying the state vector of a 6-DOF flight simulation. A convention or standard for numerical specification of unambiguous initial conditions for 6-DOF flight simulations should be developed to ensure multiple flight simulation tools start at exactly the same planet-relative position, velocity, attitude and angular rates. A significant portion of this exercise was spent resolving misinterpreted initial conditions despite an attempt to specify this information. Questions regarding whether an angular rate initial condition was with respect to a rotating Earth or to an inertial axis were raised multiple times, as well as ambiguity of initial angular attitude. Such as a standard for initial state vector description should employ ANSI/AIAA S-119-2011 for identifying simulation parameters, for ease of collaboration, and dynamic model data exchange.
7. In the atmospheric check cases, every simulation examined eventually matched trajectories with at least two other simulations to a reasonable degree, where the correlation level is a function of the simulation purpose.
8. In general, the orbital cases (implemented in at least three different simulation tools) matched fairly well, but minor differences are apparent.
9. In general, the atmospheric cases did not match as well as the orbital cases. Atmospheric flight is non-linear, due to forces and moments being related to the square of the air-relative vehicle velocity, and to other non-linear aerodynamic effects. The larger number of simulation tools applied to the atmospheric check cases increased the chances of mismatches.
10. The amount of effort required to develop, specify, and reconcile differences for multiple vehicle models across an array of simulation tools was grossly underestimated.
11. The comparison check-cases examined form the basis of a comprehensive set of verification data sets for 6-DOF flight simulations. Additional scenarios and results would improve the value of this process. One identified need is for supersonic maneuvering flight and atmospheric re-entry scenarios.
12. Nearly every simulation framework that participated in this exercise discovered at least one significant implementation difference/error that was modified/corrected to improve correlation with other simulation tools.
13. Some early problems with comparisons included different definitions among the simulation for similar sounding variable names in the recorded data. A structured, binary, compressed format to encode bulky time-history data (which is provided for this exercise as comma-separated-value Unicode text files at the URL identified by Ref. 3), as well as tools to manipulate this data, should be identified and/or developed and adopted to assist in sharing predicted trajectories from simulation tools. Using a CSV format was expeditious but cumbersome. Simulation comparisons would also benefit from employing ANSI/AIAA S-119-2011 for unambiguous identification of recorded parameters.

VI. References

[1]Anon.: *Flight Dynamics Model Exchange Standard*. ANSI/AIAA S-119-2011, American National Standard, Washington, DC, March 2011.

[2]Jackson, E. Bruce Shelton, Dr. Robert, et al., "Development of Verifications Check-cases for Six-Degree-of-Freedom Flight Vehicle Simulations," AIAA paper 2013-5071, *AIAA Modeling and Simulation Technologies Conference*, August 2013.

[3]Anon.: *Six degree-of-freedom (6-DOF) Flight Simulation Check Cases* http://nescacademy.nasa.gov/flightsim/index.html, NASA Engineering and Safety Center, 2014.

[4]Crues, Edwin Z.; Jackson, A. A.; and Morris, J. C.: "A Process for Comparing Dynamics of Distributed Space Systems Simulations." *Joint 2009 Simulation Interoperability Workshop*, San Diego, CA, 2009.

[5]Anon.: *Department of Defense World Geodetic System 1984*. NIMA TR8350.2, National Imagery and Mapping Agency, Washington, DC, 2000.

[6]Seidelmann, P. Kenneth. *Explanatory Supplement to the Astronomical Almanac: A Revision to the Explanatory Supplement to the Astronomical Ephemeris and the American Ephemeris and Nautical Almanac*. Sausalito, Calif: University Science, 2006.

[7]Anon.: *US Standard Atmosphere 1976*. NASA-TM-X-74335, Joint NOAA, NASA, and USAF publication, Washington, DC, 1976.

[8]Jackson, E. B.: "Dynamic Aerospace Vehicle Exchange Markup Language." *AIAA Modeling and Simulation Technical Committee*, version 2.0.2 ed., July 2011. Available from http://daveml.org.

[9]Jackson, E. Bruce, Shelton, Dr. Robert A., et al., "Check-cases for Verification of Six-Degree-of-Freedom Flight Vehicle Simulations," NESC-RP-12-00770, 2014.